Agricultural and Forest Meteorology 372 (2025) 110682

Contents lists available at ScienceDirect

Agricultural and Forest Meteorology

journal homepage: www.elsevier.com/locate/agrformet

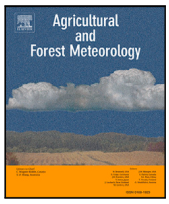

Future glacier retreat and forest expansion in the Swiss Alps provide limited benefits for carbon sinks

Fuxiao Jiang [a,*], Simone Fatichi [b], Gianalberto Losapio [a,c], Nadav Peleg [a,d]

[a] Institute of Earth Surface Dynamics, University of Lausanne, Lausanne, 1015, Switzerland
[b] Department of Civil and Environmental Engineering,National University of Singapore, Singapore, 117576, Singapore
[c] Department of Biosciences, University of Milan, Milan, 20133, Italy
[d] Expertise Center for Climate Extremes, University of Lausanne, Lausanne, 1015, Switzerland

ARTICLE INFO

Keywords:
Carbon sink
Ecohydrology
Future climate
Glacier retreat
Plant growth
Soil nutrients

ABSTRACT

Glacier retreat as a consequence of climate change creates new ice-free terrain and soil development that prompt plant colonization and ecological succession. These processes impact terrestrial ecosystems with profound ecological and societal consequences. However, quantification of how the carbon cycle evolves in deglaciated areas in response to these processes remains limited. We examined the impacts of forest expansion and soil development on the carbon cycle under climate change in a deglaciated area in the Swiss Alps. Using the mechanistic ecohydrological T&C model, we computed the changes in vegetation, soil, and carbon from 1981 to 2099 under climate change, revealing complex carbon cycle responses in deglaciating ecosystems. Vegetation growth, soil organic matter, and plant nutrient uptake are projected to increase by mid-century and then stabilize, indicating that plant growth is relatively limited by nutrient availability. The amount of carbon stored in plant biomass will increase toward the end of the century at a faster rate than that of carbon stored in soil and litter. The carbon cycle is projected to continue its current accelerating trend characterized by enhanced vegetation photosynthesis, increased plant and soil respiration, and higher net ecosystem production (NEP) by mid-century. Alpine ecosystems have already been serving as carbon sinks and have the potential to increase their carbon sink capacity, but at varying rates depending on how climate will evolve: NEP will stabilize around 24 gC m^{-2} y^{-1} in RCP4.5 or might elevate to 55 gC m^{-2} y^{-1} by end-century in RCP8.5. Even under the most extreme scenario, this increase in stored carbon in the proglacial areas of the Swiss Alps is still a drop in the ocean, as it represents only 0.9% of overall Swiss carbon emissions, thus highlighting the need for additional carbon management and mitigation efforts.

1. Introduction

Terrestrial ecosystems play a crucial role in the global carbon cycle, annually exchanging a large amount of CO_2 with the atmosphere (Schimel, 1995; Piao et al., 2009). Currently, averaged globally for the decade 2013–2022, they function as net carbon sinks, absorbing 2.5–4.1 Gt C y^{-1} of carbon from the atmosphere (Friedlingstein et al., 2025). But continued climate change heightens the risk of releasing carbon stored in the terrestrial biosphere back into the atmosphere, and has already transformed some ecosystems from sinks to sources (Peñuelas et al., 2017; Wang et al., 2020; Ke et al., 2024). Thus, monitoring ecosystem carbon cycle patterns and evolution is essential to climate change prediction and impact assessment.

Terrestrial carbon exchange directly depends on environmental factors, mainly climatic conditions (Stuart Chapin III et al., 2009). For example, surface warming has increased vegetation productivity in the high northern latitudes since the 1980s (Lucht et al., 2002; Zhu et al., 2016; Dang et al., 2023). Still, this increase could be inhibited or even reversed with a further increase in temperature toward the end of the century due to increasing aridity (Zhang et al., 2022). Considering precipitation changes, there is evidence for a robust vegetation productivity response to mean precipitation and less so to other characteristics of rainfall, such as rainfall intensity, intermittency and interannual variability (Fatichi and Ivanov, 2014; Knapp et al., 2017; Paschalis et al., 2020; Moustakis et al., 2022). Furthermore, numerous numerical experiments have explored the response of terrestrial ecosystems to elevated CO_2, nitrogen deposition, and nutrient limitations at local and global scales (De Kauwe et al., 2013; Zaehle et al., 2014; Fatichi et al., 2016b).

So far, the climatic and environmental changes that occurred since the 1960s have pointed to a global increase of terrestrial carbon

* Corresponding author.
E-mail address: fuxiao.jiang@unil.ch (F. Jiang).

https://doi.org/10.1016/j.agrformet.2025.110682
Received 12 November 2024; Received in revised form 28 May 2025; Accepted 2 June 2025
Available online 12 July 2025

sinks (Friedlingstein et al., 2025). Among terrestrial ecosystems, forest ecosystems play a critical role in the global carbon cycle, with a global forest sink of 3.5 Pg C y^{-1} (Pan et al., 2024). As a result of climate change and anthropogenic activities, these systems can evolve over time. For example, forests can naturally regenerate in deforested tropical regions and areas where agriculture has been abandoned, greatly contributing to carbon sinks (Hooker and Compton, 2003; Kuemmerle et al., 2011; Voicu et al., 2017; Williams et al., 2024). While tropical and deforested areas receive much attention, the response of the ecosystem carbon cycle to climate change in fast-changing environments, such as where glaciers are rapidly retreating and forests are taking over, has received less attention and can represent a hotspot of carbon accumulation.

Mountain regions like the Swiss Alps are warming faster than other land areas and the global average (Rangwala and Miller, 2012). Ecosystems in the Alps have already shown a high sensitivity to changing environmental conditions and are expected to be highly vulnerable to future climate change (Pörtner et al., 2022). For example, glaciers have been receding since the 1850s (Zemp et al., 2006), which leads to the establishment of terrestrial ecosystems (Bosson et al., 2023), and are projected to diminish by 50% by 2100 (Zekollari et al., 2019). Annual runoff from glacier melting reached a maximum around 2006 and has since been steadily declining (Huss and Hock, 2018), leading to glacier melt-deficit droughts (Brunner et al., 2023). This water deficit, together with robust evidence of a reduction in water availability due to snow cover loss (Rumpf et al., 2022), has the potential to considerably affect the local fauna and flora (Losapio et al., 2021; Tu et al., 2024). The shift in the terrestrial environments not only affects the hydrological cycle but also has substantial biogeochemical and ecological implications (Bosson et al., 2023), including alterations of the carbon cycle in the Alps.

Glacier retreat exposes new terrain for soil development (Musso et al., 2020), accompanied by plant colonization and succession in the deglaciated area (Fischer et al., 2019). This can lead to fast vegetation expansion as reported in the European Alps where rapid growth of forests was detected (Thom and Seidl, 2022), providing space for storage of organic carbon (Trautmann et al., 2023), and thereby increasing carbon fluxes. Soil formation related to glacier retreat has been one of the carbon sinks and increases over time, mainly accumulating carbon as soil organic carbon (SOC) (Dümig et al., 2011; Khedim et al., 2021). Warming and earlier starting of the growing season favors spring CO_2 assimilation (Rogger et al., 2022). This higher rate of storing more carbon leads to an increased net ecosystem carbon balance, which has accelerated exponentially over the past decades in glacier forelands (Smittenberg et al., 2012). While many studies have focused on soil carbon accumulation in glacier foreland ecosystems (Egli et al., 2010; Dümig et al., 2011; D'Amico et al., 2015; Khedim et al., 2021; Xing et al., 2022; Liu et al., 2024), there is still limited understanding of the full carbon cycle in these ecosystems. Although a shift toward higher carbon storage is observed in soils over time (Egli et al., 2010; Dümig et al., 2011; D'Amico et al., 2015), the complete carbon cycle, including other carbon pools and their future capacity to increase sink capabilities, is not fully understood yet. Elucidating whether glacier-related ecosystems currently act as carbon sinks, or if they will become carbon neutral or even carbon sources in the future is crucial to ecosystem management and to inform climate change mitigation actions.

Here, we assess and characterize the joint impact of climate change and glacier retreat on carbon dynamics considering soil development and forest expansion. To this end, our numerical modeling focuses on a fast-retreating alpine glacier in Switzerland as a case study. We employ a weather generator model to enable climate simulations at an hourly scale and estimate how climate uncertainties cascade into carbon flux estimations on a glacier foreland in the Ferpècle catchment, Swiss Alps. Invoked by two greenhouse gas emission scenarios obtained from climate models, the generated climate forcings then drive a mechanistic ecohydrological model to compute the time series of carbon uptake and storage from 1981 to 2099. We address the following research questions: how do carbon storage and carbon balance vary with ecological succession and soil development? Which environmental factors control the variations in carbon balance in deglaciating ecosystems? As a final point, we discuss the potential contribution of proglacial areas to carbon absorption in the Alpine domain at the national scale, considering Switzerland's objective to reach net-zero emissions by 2050.

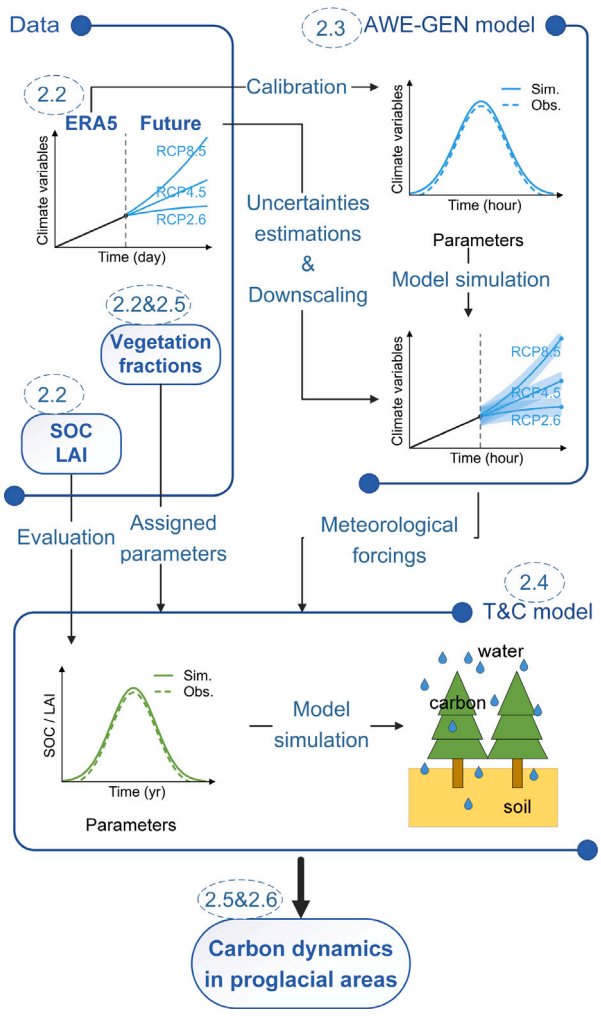

Fig. 1. A flowchart describing the data and methods employed to assess changes in the carbon cycle due to soil and vegetation dynamics following glacier retreat under climate change. The number next to each data or process refers to the relevant sections.

2. Study area, data, and methods

The present and future carbon dynamics in the Ferpècle proglacial area were investigated in several steps illustrated in Fig. 1. Information on the present and future climates was first collected and fed into a weather generator model to generate multiple realizations of downscaled present and future hourly climate time series, which were later used to quantify uncertainties associated with future carbon storage. These climate time series were subsequently employed to drive a mechanistic ecohydrological model to analyze the changes in carbon pools and fluxes. In the following, a detailed description of the study area, data, and models used is presented.

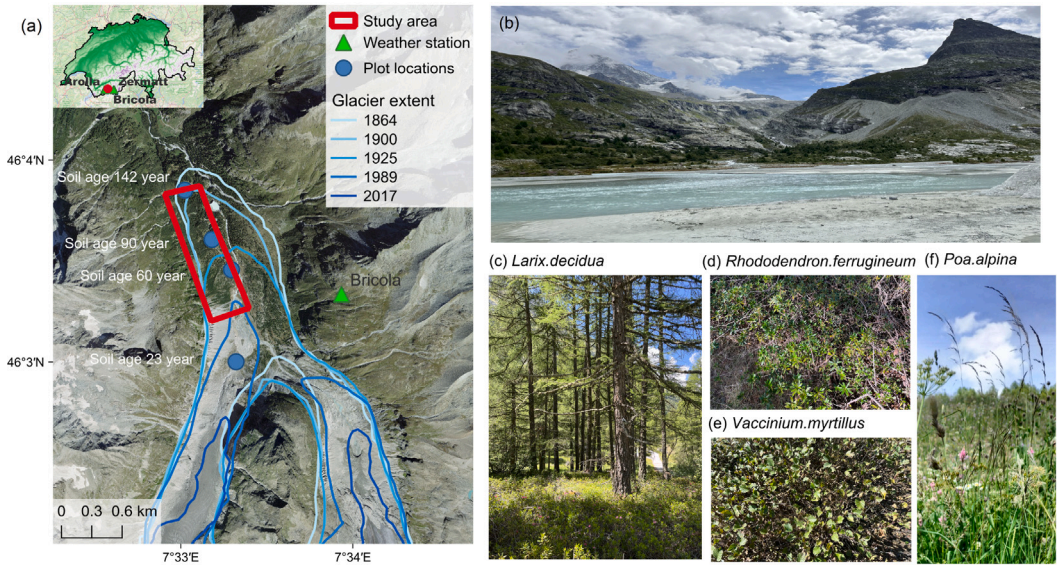

Fig. 2. The Ferpècle catchment in the Swiss Alps: (a) location and (b) landscape; main species in this catchment: (c) *Larix decidua*, (d) *Rhododendron ferrugineum*, (e) *Vaccinium myrtillus*, and (f) *Poa alpina*.

2.1. Study area

We focused our numerical experiments on the proglacial ecosystems of the Ferpècle catchment, Swiss Alps (Fig. 2a). This area consists of several glacier forelands, where substantial proglacial activities occur, resulting from the retreat of two main glaciers: Ferpècle and Mont Minè. During the Little Ice Age, these two glaciers coalesced, occupying the entire Ferpècle catchment up to around 1800 m a.s.l (see their extents in Fig. 2a) (Lambiel, 2021). They separated in the early 1960s, although glacier retreat was briefly interrupted by a short period of growth in the 1970s and 1980s (Lambiel, 2021). Between 1973 and 2023, the glaciers receded by 1274 m, losing 17.5% of their size. The Ferpècle catchment is an ideal study area due to its well-monitored glacier retreat activities, ongoing biodiversity monitoring, and its representation of a typical fast retreating alpine glacier.

From the current glacier position to the former frontal Little Ice Age's position, the moraine shows clear evidence of typical spatio-temporal evolution of soil development, plant colonization, and ecological succession (Lambiel, 2021). The study area is dominated by the Arolla gneiss, a coarse-grained metamorphic rock primarily composed of quartz, feldspar, and mica. In addition to Arolla gneiss, other metamorphic rocks present include eclogites, serpentinites, and calcschists. The main soil type is Leptosols, dominated by coarse mineral fractions (sand and gravel) with minimal clay content at its early development stage. It is generally thin and rocky, consisting of glacial till, weathered metamorphic material, and morainic deposits. Plant diversity initially increased after glacier retreat, along with an increase in soil organic matter (SOM) and soil nutrients (Charles et al., 2024). Over more than 120 years, the soil acidified, the carbon to nitrogen (C/N) ratio rose, and plant diversity and composition changed. Pioneer herbaceous plants were quickly replaced by coniferous forests (Charles et al., 2024). The main plant species are *Larix decidua* (trees; a European larch), *Rhododendron ferrugineum* (evergreen shrubs; alpenrose), *Vaccinium myrtillus* (deciduous shrubs; European blueberry), and *Poa alpina* (grass; alpine bluegrass), occupying 13.1%, 8.1%, 6.1%, and 32.7% of the study area, respectively (Table S5 and Fig. 2c–f).

2.2. Data

Climate variables representing the present climate (1959–2022) were obtained from the ERA5 hourly climate reanalysis product (Hersbach et al., 2020) to estimate the parameters of the AWE-GEN model (Section 2.3) and run the T&C model (Section 2.4). Data include time series of cloud cover, precipitation, atmospheric pressure, near-surface relative humidity, shortwave radiation, near-surface air and dewpoint temperatures, and 2-m wind speed, and were derived from the grid cell covering the study area (45.9–46.1 °N and 7.4–7.6 °E). Due to its large geographic coverage, ERA5 data needed to be bias-corrected using local observations (Alves et al., 2021). To that end, we collected climatic data from MeteoSwiss automatic weather stations located in the vicinity of the Ferpècle catchment: precipitation from the Bricola station, air and dewpoint temperatures and wind speed from the Arolla station, and shortwave radiation from the Zermatt station (see the location of the stations in Fig. 2a) for the corresponding period.

Future climate (precipitation and air temperature) data were obtained from 10 regional climate models (RCM) that compose the official CH2018 climate scenarios for Switzerland (Fischer et al., 2022). Data cover the 1981–2099 period and include both the historical simulations as well as two greenhouse gas emission scenarios (RCP4.5 and RCP8.5). In addition, observed and projected atmospheric CO_2 concentrations were also derived from two sources: historical data for the period 1959–2014 from the CMIP6 product (Meinshausen et al., 2017), and future data for the period 2015–2099 from Cheng et al. (2022).

Vegetation fractions were obtained from the Swiss Federal Statistical Office for the years 1985, 1997, 2009, and 2018 (Table S5). Soil organic carbon (SOC) content was determined using a CHNS Elemental Analyser for soil samples collected from the top 10 cm of soil after removing stones (>5 cm) and the organic layer, expressed as a percentage of the initial, oven-dried soil mass (Charles et al., 2024), and was converted to units of carbon per area (Section S1). Sentinel-2 L2 A data were downloaded to retrieve leaf area index (LAI) with a high spatial resolution of 30 m using SNAP toolbox (Weiss et al., 2016).

2.3. The AWE-GEN model

The stochastic Advanced WEather GENerator (AWE-GEN) model (Ivanov et al., 2007; Fatichi et al., 2011) combines physical information and statistical approaches to reproduce a comprehensive and realistic set of meteorological times series at the hourly resolution, including precipitation, air temperature, cloud cover, relative humidity, wind speed, and solar radiation. The model captures the diurnal cycle and properly represents extreme climatic events such as heavy precipitation, and therefore can be used to downscale and bias-correct climate reanalysis data available at coarser resolution to a local scale (Fatichi

et al., 2021; Ramirez et al., 2023). AWE-GEN can be also used to adequately describe the natural climate variability (also known as internal or stochastic climate variability) through the simulation of a large ensemble of realizations for a given climate (Fatichi et al., 2016a). Furthermore, AWE-GEN can be re-parameterized to simulate future climate using factors of change obtained from climate models (Fatichi et al., 2013), thus allowing the investigation of how climate change impacts future eco-hydrological systems and the quantification of their uncertainties (Moustakis et al., 2022).

2.4. The T&C model

The Tethys-Chloris (T&C) model (Fatichi et al., 2012) is an hourly-scale mechanistic ecohydrological model that simulates the exchanges of water, energy, and carbon among the atmosphere, vegetation, and soil. It is a grid-based model that can be implemented from a single plot (Fatichi et al., 2014) to the catchment and to large regional scales (e.g., Mastrotheodoros et al. (2020)). The vegetation components can accommodate horizontal and vertical composition of vegetation to replicate the coexistence of high- (i.e., trees) and low-vegetation (shrubs and grass) layers. The vegetation dynamics describe the plant life cycle including photosynthesis at the hourly scale and phenology, carbon allocation, and tissue turnover at the daily time scale. The soil column can be partitioned into multiple layers to solve for infiltration, ground evaporation, root water uptake and more generally for variably saturated flow dynamics. The model also well represents hydrological fluxes and energy fluxes, such as net radiation, latent and sensible heat fluxes (Fatichi et al., 2012; Mastrotheodoros et al., 2017; Manoli et al., 2018; Botter et al., 2021; Paschalis et al., 2024). The T&C model has been extensively calibrated and validated in Alpine environments (Fatichi et al., 2014; Mastrotheodoros et al., 2019, 2020; Botter et al., 2021) (Table S4) and we have used a similar parameterization as that previously reported.

Given the vital importance of soil properties (e.g., soil carbon, and soil nutrients) in the ecosystem carbon cycle, this study explicitly considers the soil biogeochemistry (BG) module (Fatichi et al., 2019). This module possesses various components, including litter generation and turnover, the carbon and nutrient budgets of litter and soil organic matter subdivided into functional components, soil macrofauna, and the supply of primary minerals through rock weathering. The biogeochemical fluxes are solved at a daily time scale. The T&C-BG model has been employed to quantify changes in grassland productivity in a changing climate in the Alps (Botter et al., 2021) and China (Pang et al., 2023). Here, we used it to explore the responses of the ecosystem carbon cycle under different climate scenarios in the Swiss Alps as explained in the experimental design.

2.5. Experimental design

This section describes how AWE-GEN and T&C models were set up to simulate carbon storage for present and future climates. First, the ERA5 data from 1959 to 2022 were bias-corrected based on the observed data from the weather stations: precipitation was adjusted by applying a quantile mapping method, air and dewpoint temperature were de-biased using a delta monthly differences approach, and wind speed and shortwave radiation were bias-corrected considering the ratio between the observed and ERA5 data. Relative humidity was calculated using the bias-corrected air and dewpoint temperature along with atmospheric pressure, as ERA5 hourly data on single levels do not provide relative humidity directly. The bias-corrected data was driven T&C model without deactivating the BG module to adjust vegetation parameters based on values from previous studies (e.g., Mastrotheodoros et al. (2020) and Botter et al. (2021)). Then, these time series were repeated to extend them into a single realization of one thousand years representing the statistics of the present climate. We ran the T&C model with this extended period to enable soil nutrient accumulation from a starting point of minimal soil carbon concentration in the study area. Exploring different soil parameter sets, we found the best one (Table S6) that mimicked the measured SOC and its changing rates.

We defined the reference climate as the period between 1981 and 2010. Our rationale for choosing this period is that we require a 30-year continuous climate data block to conduct robust statistical analysis, as well as that the Swiss official CH2018 scenarios, used later to look at future periods, are beginning in 1981. The AWE-GEN model was calibrated for this period using the bias-corrected ERA5 data. The remaining ERA5 data for the years 2011–2022 were used to validate the AWE-GEN model's ability to simulate meteorological variables.

To simulate the future period (2011 to 2099) with the AWE-GEN model, we divided this timeframe into nine overlapping sub-periods, each spanning three decades (i.e., 1991–2020, 2001–2030 ... 2071–2100), and employed the factors of change (FC) approach (Fatichi et al., 2013) to compute the changes in statistics of precipitation and air temperature for these sub-periods in comparison with the reference period. Factor of change for precipitation (FC_{Pr}) was calculated on a monthly basis:

$$FC_{Pr} = \frac{Pr_{month}^{RCM,FUT}}{Pr_{month}^{RCM,REF}}, \tag{1}$$

where $Pr_{month}^{RCM,FUT}$ is the monthly precipitation statistic from a given regional climate model (RCM) from the CH2018 climate scenarios for a given future period (FUT), and $Pr_{month}^{RCM,REF}$ is the monthly precipitation statistic from a given RCM for the reference period (REF). In the case of air temperature, FC_{Ta} was calculated in a similar manner, but taking into account the difference in mean monthly air temperature instead of the ratio:

$$FC_{Ta} = Ta_{month}^{RCM,FUT} - Ta_{month}^{RCM,REF}. \tag{2}$$

We note that the FC approach can account for changes in higher-order statistics than simply the mean (e.g., standard deviation, kurtosis) (Peleg et al., 2019), and even if only the mean is altered, it will cascade to impact other statistical aspects of the climate variable in question, such as its extremes (Fatichi et al., 2013).

For each future sub-period, the 10 RCMs yielded 10 sets of FC applied to the ERA5 data to obtain modified climate statistics representative of possible future pseudo-climates. Then, we re-calibrated AWE-GEN and estimated its parameters across the nine future sub-periods. To account for the uncertainties of future climate projections, we ran AWE-GEN to stochastically simulate 10 realizations for each of the reference and future periods (representing the natural climate variability), for each of the two climate scenarios (emission scenario uncertainty), and for each of the 10 RCMs (climate model uncertainty) (Fatichi et al., 2016a). This resulted in a large ensemble consisting of 100 realizations for each emission scenario spanning from 1959–2099. The FC for mean precipitation and mean air temperature and the 5–95th percentile range of the large ensemble are presented in Fig. 3.

The climate ensemble was used to drive the T&C model. The simulations were launched from 1959 to 1980 as a spin-up period, but the outputs for this period were considered initialization and discarded. The T&C model also required inputs of the projected changes in vegetation fractions in the study area, which were predicted by linear models. First, soil chemical composition and physical components in the last several decades were analyzed through principal component analysis (Fig. S1), identifying two dominant factors that affect vegetation fractions, which is the time since glacier retreat (ice-free years) and the C/N ratio. Then, based on the time series of these two dominant factors and the monitored vegetation fractions (Table S5), linear models were set:

$$f_{forest} = 0.0036 \cdot x_{time} + 0.015 \cdot x_{C/N_{forest}} - 5.2 \cdot 10^{-6} \tag{3}$$

$$f_{grass} = e^{-0.01 \cdot x_{time} + 0.63 \cdot x_{C/N_{grass}} - 6.8}, \tag{4}$$

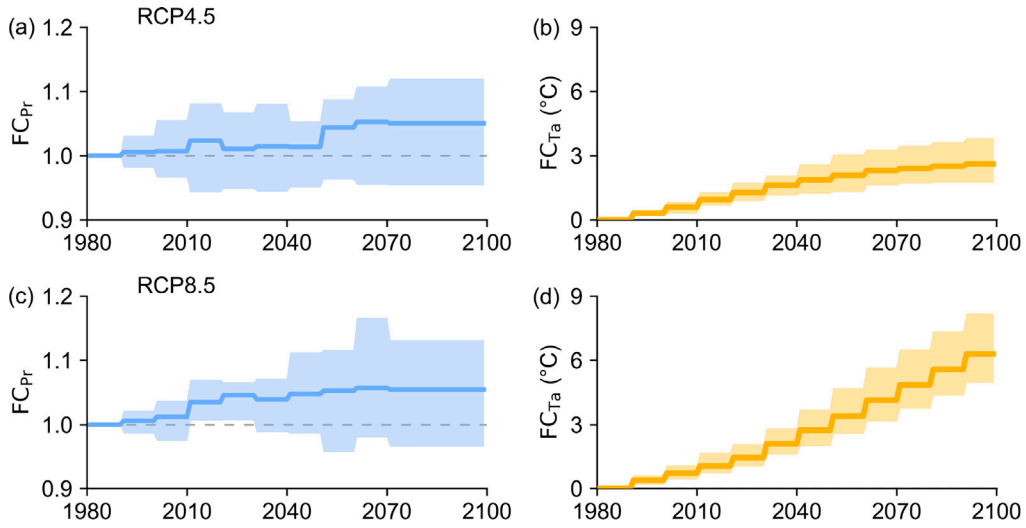

Fig. 3. (a) Factor of change for mean precipitation (FC_{Pr}, blue line) with its 5–95th percentile range (shaded area) for RCP4.5, (b) factor of change for mean temperature (FC_{Ta}, orange line) with its 5–95th percentile range (shaded area) for the RCP4.5 scenario. (c) and (d) are the same as (a) and (b) but for RCP8.5.

$$f_{bare} = e^{-0.023 \cdot x_{time} + 0.03}, \tag{5}$$

$$f_{eveS} = 0.57 \cdot (1 - f_{forest} - f_{grass} - f_{bare}), \tag{6}$$

$$f_{decS} = 0.43 \cdot (1 - f_{forest} - f_{grass} - f_{bare}), \tag{7}$$

where f_{forest}, f_{grass}, f_{bare}, f_{eveS}, and f_{decS} are the fractions of the area covered by the forest, grass, bare land, evergreen and deciduous shrubs (respectively), x_{time} is the ice-free years, $x_{C/N_{forest}}$ and $x_{C/N_{grass}}$ are the C/N ratios of forest and grass (respectively). To project the future vegetation fractions, we extrapolated these linear relations to the future, and the future C/N ratios were derived from the T&C model simulations.

To investigate the spatial heterogeneity of the ecosystem carbon cycle in response to the dynamics of vegetation cover and soil development, four distinct locations along a chronosequence were selected, representing soil ages of 23, 60, 90, and 142 years of 2022 (Fig. 2a). These sites capture the transitions from recently deglaciated areas to more developed ones, allowing for an assessment of how the ecosystem carbon cycle evolves with soil formation and vegetation succession using the T&C model. The simulations started in 2022, aligning with the determination of soil ages in that year.

Last, a sensitivity analysis was conducted to assess the factors controlling the variations in carbon uptake and storage. The control scenario (CT) referred to the ensemble run as described above, i.e., including the time series of the present and projected precipitation, air temperature, and atmospheric CO_2 concentration with the BG module activated in the T&C model. The additional scenarios included: STa – no changes in air temperature (i.e., FC_{Ta} was not applied and air temperature retained the same as the 1981–1990 period in the future climate); SPr – no changes in precipitation in the future; SCO2 – no changes in atmospheric CO_2 concentration, with current concentration levels maintained; SBG – the BG module was deactivated (i.e., soil biogeochemistry processes did not play a role in plant growth and physiology, and plants were considered in equilibrium with their nutrient environment) while all other climate variables were changed. We quantified the differences in carbon uptake at the end of the simulations between the control and the other four scenarios to mark the relative contribution of each factor. In the sensitivity analysis, we used net primary production (NPP) instead of net ecosystem production (NEP, see next) to represent carbon uptake by plants, as NEP cannot be computed when the BG module was deactivated.

Table 1
Summary of the sensitivity analysis scenarios. Plus symbols indicate that future climate scenarios have been included in the simulation, while "current levels" indicate that the variable is maintained at the same level as in 1981–1990. Check marks indicate soil biogeochemistry processes (BG module) play a role in plant growth and physiology, but "Deactivated" indicates plants are considered in equilibrium with their nutrient environment.

Scenario	Ta	Pr	CO_2	BG module
CT	+	+	+	✓
STa	Current levels	+	+	✓
SPr	+	Current levels	+	✓
SCO2	+	+	Current levels	✓
SBG	+	+	+	Deactivated

2.6. Metrics for ecosystem carbon balance

Net ecosystem production (NEP) measures an ecosystem's net carbon accumulation rate (terrestrial biomass, soil organic matter, and litter), where positive values indicate that the ecosystem acts as a carbon sink. In the absence of disturbances and lateral C transport, NEP can be simplified as the balance between carbon gain and loss for ecosystems (Chapin et al., 2006), such as the deglaciating ecosystems:

$$NEP \approx GPP - (RA + RH), \tag{8}$$

where NEP is defined as the carbon gain that is expressed by the gross primary production (GPP), minus the total ecosystem respiration, composed of the autotrophic respiration (RA) and the heterotrophic respiration (RH).

3. Results

3.1. Models evaluation

We begin by evaluating the AWE-GEN's ability to simulate reference climate statistics and the T&C model's ability to reproduce vegetation dynamics. Here, we report the monthly comparison of the key climatic drivers affecting vegetation: precipitation, air temperature, shortwave radiation, and relative humidity. The monthly precipitation during the calibration period 1981–2010 is well reproduced by AWE-GEN (Fig. 4a), with a bias of only −0.047 mm between the mean of the simulations and bias-corrected ERA5 data. We go beyond the traditional evaluation procedure by comparing the observed ERA5 data from 2011–2022 with the simulated data of the two emission scenarios. Observations and simulations are less closely matched during

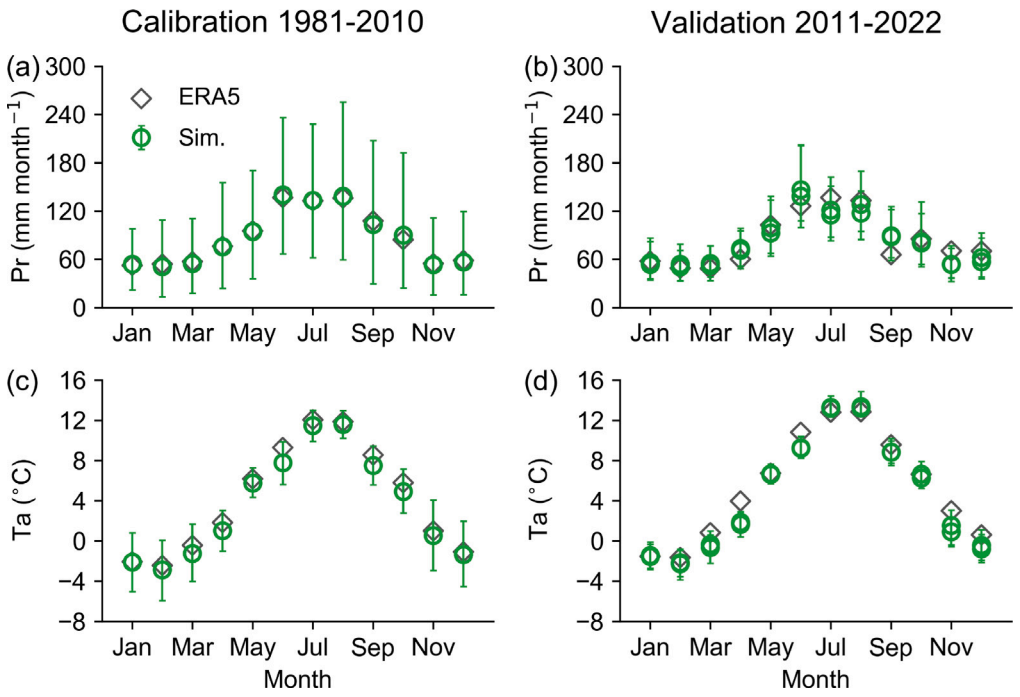

Fig. 4. Comparison of simulated monthly precipitation (a and b) and air temperature (c and d) with bias-corrected ERA5 data during the calibration 1981–2010 and validation period 2011–2022, which already includes climate perturbations with factors of change. The vertical bars represent the 5–95th percentile range.

Table 2
The measured and simulated SOC storage and accumulation rate for 0–25 cm soil depth in Ferpècle.

Soil age (y)	Measured SOC		Simulated SOC	
	Value (gC m^{-2})	Rate (gC m^{-2} y^{-1})	Value (gC m^{-2})	Rate (gC m^{-2} y^{-1})
60	2333	–	2412	–
90	3051	24	3324	30.4
142	3746	23.2	4157	27.8

this period (Fig. 4b), as expected, but the biases remain small (−1.81 mm for RCP4.5 and 0.19 mm for RCP8.5). Similarly, the monthly air temperature is highly consistent with the bias-corrected EAR5 values for both the calibration and validation periods (Fig. 4c–d). The bias in air temperature for the 1981–2010 period is as low as −0.63 °C and remains in the same order for the year 2011–2022 (−0.72 °C). Biases for shortwave radiation and relative humidity for the calibration period are also in the acceptable range of 22.99 W m^{-2} and −0.04, respectively, presented in Fig. S2.

We used the leaf area index (LAI) and soil organic carbon (SOC) to evaluate the T&C model's performance. LAI is a key variable that directly affects plant photosynthesis and respiration. Due to image quality limitations, the modeled LAI is compared to Sentinel-2 LAI data only between June and September (i.e., during the growing season) from 2019 to 2023, with mean values of 2 and 2.6 m^2 m^{-2}, respectively. The 23% difference in the simulated LAI is within a reasonable range due to uncertainties in remote sensing products, the differences in spatial resolution and the extent between the Sentinel-2 data and the study area. The measured and simulated SOC for soil depths of 0–25 cm are presented in Table 2. The simulated SOC accumulation rate is roughly consistent with the measurements, in the order of 25 gC m^{-2} y^{-1}, with an overestimation of 9%.

3.2. Vegetation dynamics

The projected changes in the fractions of bare soil and vegetation types (grass, shrubs, and forests) derived from the linear regression models are presented in Fig. 5a. While bare soil has predominated the study area in recent decades, enhanced soil development due to glacier retreat enabled vegetation to take over, reducing the fraction of bare soil below 15% already today in the study area as defined in the "red box" (Fig. 2a). A diverse mixture of shrubs gradually occupies the unvegetated areas and encroaches on grasslands. Simultaneously, coniferous forests are projected to steadily grow and shade out shrubs, leading to shrubs' decline from mid-century. Ultimately, soil and environmental conditions enable forests to quickly dominate, and are projected to reach over 75% coverage by the end of this century – a growth of 25% from the current level.

The changes in vegetation fractions and climate influence the annual and seasonal leaf area index (LAI) (Fig. 5b). Annual average LAI increases until mid-century in both climate scenarios, and then levels off under RCP4.5 to almost three times its initial level in the 1980s (i.e., an increase from 0.5 to 1.5 m^2 m^{-2}). In contrast, under RCP8.5, LAI continues to rise even after the mid-century, albeit at a slower rate, at the end of the century reaching a level that is four times higher than the 1980s.

3.3. Soil and plant nutrients

Soil organic nutrients (nitrogen and phosphorus) in mineral soils accumulate with increasing soil age (Fig. 6a). Since the 1980s, these nutrients are projected to experience a rapid build-up to continue accumulating till the end of the century under both climate scenarios, as the soil is continuously developing. Soil organic nitrogen is projected to increase by 1.5 times (from about 200 to 350 gN m^{-2}), while soil organic phosphorus will double its values (from about 40 to 80 gP m^{-2}) by the end of the century in comparison to the 1980s values (Fig. 6a). Their contents remain fairly stable throughout the year (not shown).

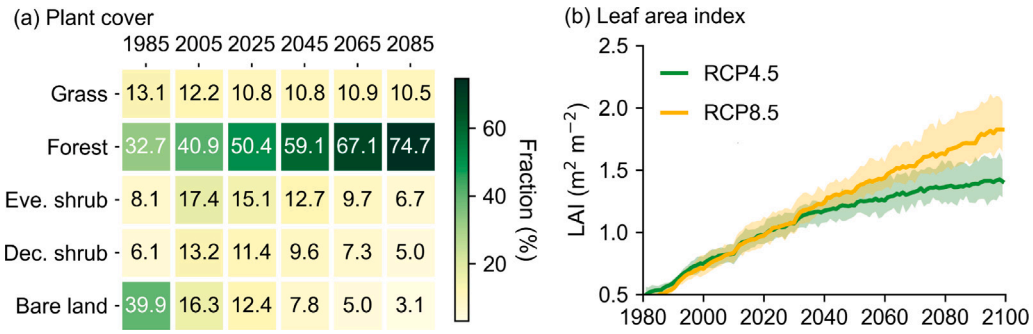

Fig. 5. (a) Vegetation fraction and (b) annual average leaf area index (LAI) during 1981–2099 under RCP4.5 and RCP8.5, respectively. Shaded areas indicate the 5–95th percentile range.

Mineral available nutrients, derived from soil inorganic nutrient pools, primarily include available nitrogen and available phosphorus (Fig. 6b). From the beginning of the simulation until the late 2030s, available nitrogen has been decreasing and then stabilizing in both climate scenarios. Conversely, available phosphorus increases considerably from 0.78 gP m^{-2} in 1980 to 1.78 gP m^{-2} in the end-century, which is a relatively high increase rate. We note that ecosystems in proglacial areas are initially limited by phosphorus at the early stages of primary succession (Göransson et al., 2016; Darcy et al., 2018). However, as soil continues to develop, the dominant nutrient limitation gradually shift toward nitrogen at the late successional stages (Yang et al., 2021; Zhang et al., 2021).

Plant uptake of mineral nutrients (nitrogen and phosphorus; Fig. 6c) is regulated by both soil organic matter decomposition, plant nutrient demand, and plant tissue nutrient concentration. Plant nutrient uptake increased equally until mid-century in both scenarios, after which it is higher in RCP8.5 than in RCP4.5. Overall, mineral available phosphorous is relatively high, likely due to a model limitation, but still the phosphorous uptake remains reasonably accurate, as this process is modulated by plants.

3.4. Ecosystem carbon cycle

After quantifying the changes in vegetation patterns and soil nutrients following glacier retreat, we investigated the evolution of the ecosystem's carbon balance. The changes in vegetation, soil (mainly refers to the mineral soil), and litter carbon pools (overlap with the organic layer) are presented in Fig. 7. Mean simulated carbon pools during 1981–2020 are 1215 (vegetation), 2684 (soil), and 857 (litter) gC m^{-2}, increasing respectively to 2014, 3693, and 1018 gC m^{-2} by mid-century for the two climate scenarios examined. After that, in the absence of disturbances, these pools exhibit contrasting patterns: vegetation carbon continues to rise rapidly (with RCP8.5 having a higher trend than RCP4.5), soil carbon increase slowly (with a similar trend in both RCPs), and litter carbon stabilizes (less under RCP4.5 than RCP8.5, probably because more decomposition at higher air temperature keeps pace with more litter production).

The temporal dynamics of the key carbon-balance variables (NEP, RH, RA, and GPP) are presented in Fig. 8. As one can expect, vegetation productivity and respiration are rising with time, but while stabilization is reached in RCP4.5 by mid-century, the positive trend continues in RCP8.5 toward the end of the century. Autotrophic respiration (Fig. 8c) is much larger than heterotrophic respiration (Fig. 8b) without considering fauna in this region as the ecosystem is still young and aggrading. Both respiration fluxes become more comparable after the mid-century in RCP4.5, but not in RCP8.5. The net carbon accumulation in the ecosystem (NEP; Fig. 8a) is positive over the whole period under both RCP scenarios, implying the ecosystem consistently functions as a carbon sink. Carbon sink levels remain largely stable for RCP4.5 (around 24 gC m^{-2} y^{-1}) but increases largely to around 55 gC m^{-2} y^{-1} by end-century for RCP8.5.

3.5. Carbon dynamics across the glacier foreland

The pronounced spatial heterogeneity of the ecosystem carbon cycle in the glacier foreland is illustrated in Fig. 9. All carbon pools have remarkable increasing trends toward the end of the century for soils younger than 60 years (Fig. 9e,f). In contrast, in soils that are longer exposed (i.e., > 90 years, Fig. 9g,h), the soil carbon and litter carbon pools remain stable from 2060 to 2099, while vegetation carbon pools rise even when approaching the end-century. Similarly, the key carbon-balance variables (RA, RH, and GPP) rise rapidly in the young parts even after mid-century (Fig. 9a,b), while they either increase slowly or stabilize in old parts of the landscape (Fig. 9c,d). However, the absolute carbon sink level increases along the chronosequence, from 18 to 58 gC m^{-2} y^{-1}, values at the end of the century (Fig. 9a–d). Except for the 23-year-old soil sites, the carbon sink capacities are relatively stable during the 2022–2099. As the very young soil only occupies a small proportion of the foreland, the dynamics presented in Fig. 9c can be considered as generally representative of carbon budget in the study area.

4. Discussion

4.1. Ecosystem carbon cycle changes following glacier retreat

The simulations presented here show that fast forest expansion will result in considerable changes to the carbon stocks (Fig. 7), with the greatest changes potentially occurring in vegetation pools (Fig. 7a) that are projected to reach 5 kg m^{-2} by end-century under the RCP8.5 scenario. Although our estimates are for relatively young, still-growing forests, they are consistent with those expected for mature Alpine forests. In mature mixed larch forests in the Alps, vegetation excluding coarse roots can store carbon between 6.61 and 16.3 kg m^{-2} (Risch et al., 2008; Nagler et al., 2015; Brändli et al., 2020; Canedoli et al., 2024), indicating that forest carbon intake can be further increased in the study area. We show that litter carbon pools largely overlap with the organic layer, increasing from 0.6 to 1 kg m^{-2} over time – while in mature larch forests, carbon in the organic horizons can have even higher capacity, ranging from 0.71 to 4.76 kg m^{-2} (Nagler et al., 2015; Canedoli et al., 2024). The simulated content of soil carbon stocks is between 6.5 g C kg^{-1} (for soil aged 50-year) to 13.3 g C kg^{-1} (soil aged 140-year), which is consistent with other studies in the Alps (Egli et al., 2010; D'Amico et al., 2015). Moreover, in our simulations, in the successional forest, carbon stocks in living biomass are lower than in soil but increase with time due to enlarged tree biomass (Fig. 7), and absence of simulated major disturbances, which aligns with values reported in other studies (Thuille and Schulze, 2006; Hiltbrunner et al., 2013; Guidi et al., 2014). Also, litter carbon pools level off after mid-century, but soil carbon increases slowly, as sites for storing physiochemically protected mineral associated organic carbon might decrease, especially in a coarse texture soil, preventing faster SOC content changes (Fang et al., 2015).

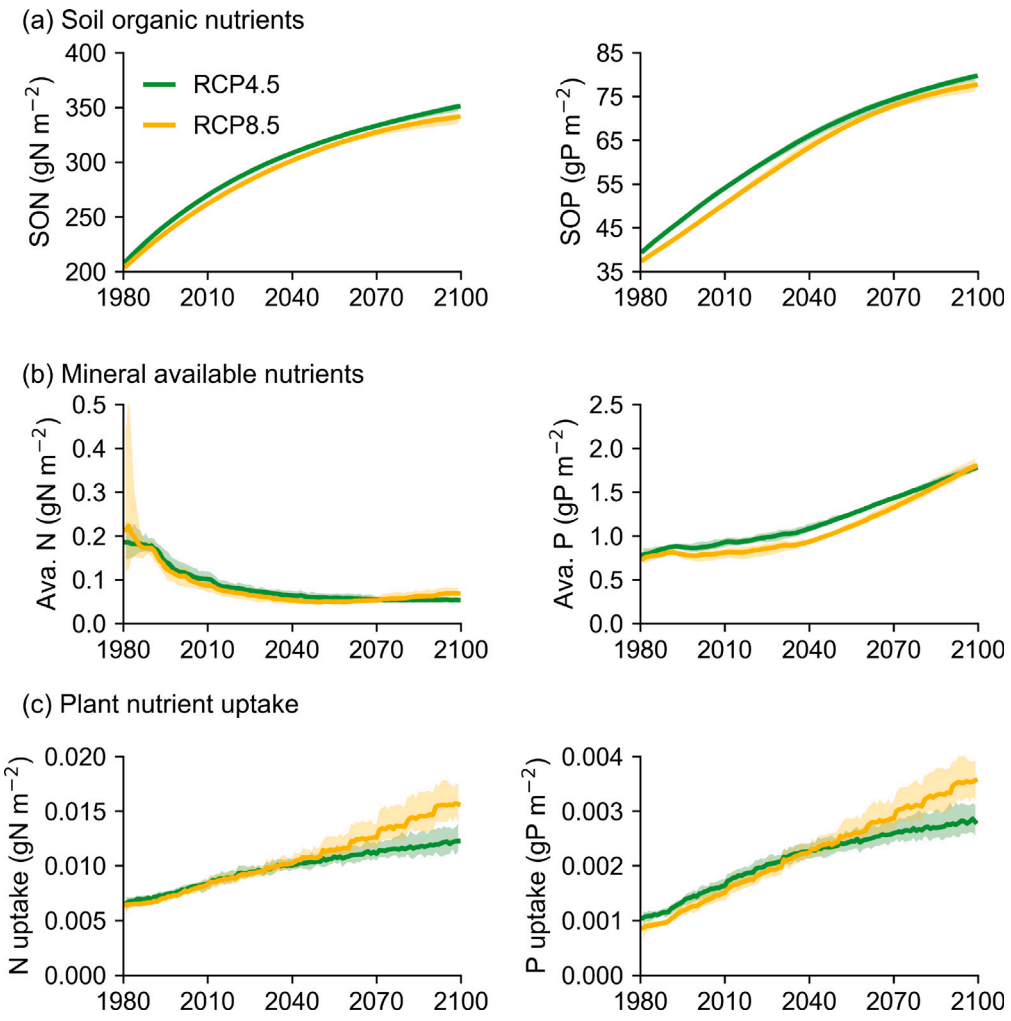

Fig. 6. Annual changes in (a) soil organic nutrients: soil organic nitrogen (SON) and soil organic phosphorus (SOP), (b) mineral available nutrients: available nitrogen (Ava. N) and available phosphorus (Ava. P), and (c) plant nutrient uptake: *N* uptake and P uptake during 1981–2099 under RCP4.5 (green lines) and RCP8.5 (yellow lines). Shaded areas indicate the 5–95th percentile range.

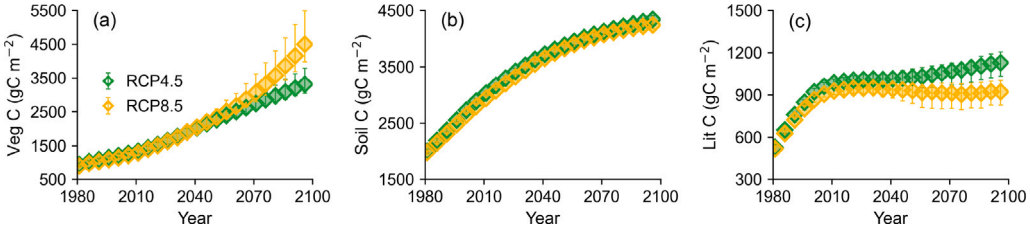

Fig. 7. Annual values of: (a) vegetation carbon pools (Veg C), (b) soil carbon pools (Soil C), and (c) litter carbon pools (Lit C) during 1981–2099 under RCP4.5 and RCP8.5. Vertical bars represent the 5–95th percentile range.

Plant photosynthetic rates have been increasing equally under different climate scenarios until mid-century, after which they vary as higher warming promotes larger GPP that leads to higher leaf area, promoting GPP increase even further (Street et al., 2007; Li et al., 2019). Although both GPP and RA have upward trends, plant carbon use efficiency (CUE), which is one minus the ratio of RA to GPP (Manzoni et al., 2018), exhibits a slight downward trend under both scenarios. This is because CUE tends to decrease with forest ages and even more so with air temperature (Delucia et al., 2007; Luo et al., 2025). Carbon loss from heterotrophic respiration is increasing with warming, driven by higher litter inputs, greater microbial biomass, and overall higher litter decomposition at higher temperatures (Wang et al., 2014; Nissan et al., 2023). Using our simulations, soil respiration, excluding aboveground litter respiration, at mature soils (> 110 years) was estimated to be about 200 gC m^{-2} y^{-1} (Fig. 8b), comparable to 160 g CO_2-C m^{-2} y^{-1} in the nearby Damma glacier foreland (Guelland et al., 2013). When warming stimulates vegetation productivity more than litter decomposition and SOM oxidation in an ecosystem, carbon storage increases, forming a carbon sink (Cao and Woodward, 1998). The carbon sink rate of 24 gC m^{-2} y^{-1} (RCP4.5, Fig. 8a) in Ferpècle proglacial area coincides with other findings, such as the Swiss Damma (Smittenberg et al., 2012) and Norwegian Brøgger (Nakatsubo et al., 2005) glacier forelands, where carbon accumulated approximately 20 gC m^{-2} y^{-1}. Under RCP8.5, the carbon sink rate gets larger

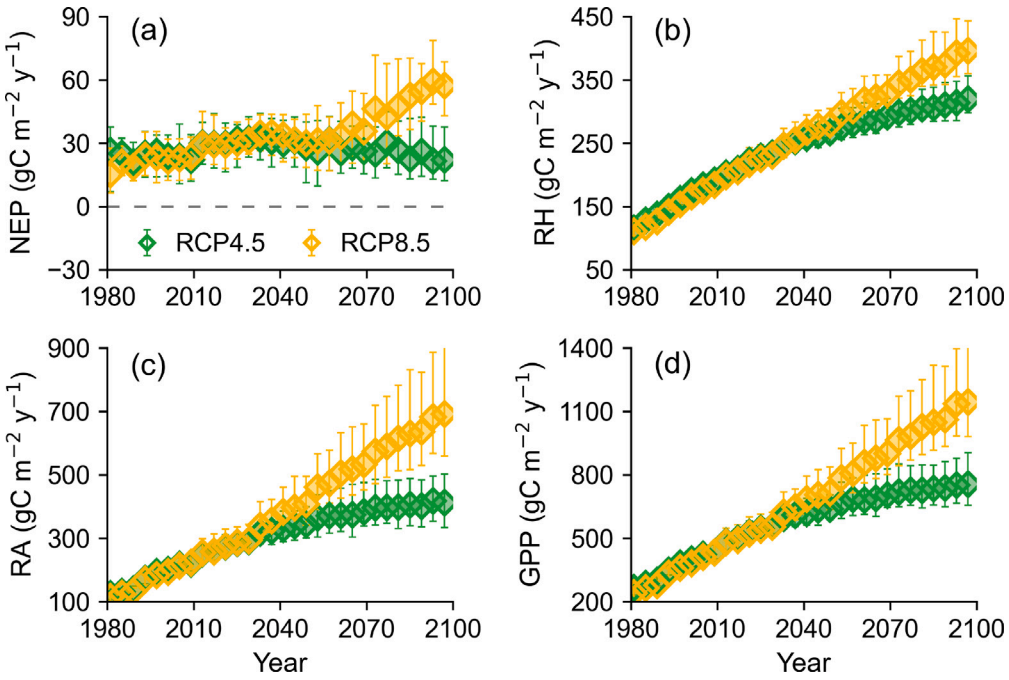

Fig. 8. Annual carbon balance: (a) net ecosystem production (NEP), (b) heterotrophic respiration (RH), (c) autotrophic respiration (RA), and (d) gross primary production (GPP) during 1981–2099 under RCP4.5 and RCP8.5. Vertical bars indicate the 5–95th percentile range.

at 55 gC m^{-2} y^{-1}, as a result of air temperature and CO_2 concentration stimulating forest growth in these expanding ecosystems.

4.2. Driving mechanisms

Exploring the response of the ecosystem carbon cycle to changing environmental conditions (Fig. 10), we discover that increasing air temperature dominantly enhances carbon sink levels in glacier foreland ecosystems, contributing to a 28% increase in NPP (Fig. 10a,b). This is likely attributed to earlier snowmelt and a longer growing season (Rogger et al., 2022), which supports higher LAI to sustain productivity (Li et al., 2019). In comparison, elevated atmospheric CO_2 concentrations only account for 6% of NPP increase, with soil nutrient limitations suppressing CO_2 fertilization effects (Fleischer and Terrer, 2022). Since these regions do not experience water scarcity (Filippa et al., 2019), precipitation changes have a negligible impact on NPP increase. In contrast, soil nutrient limitations directly result in a 42% change in NPP, which indicates that nutrients play a key role in improving carbon sinks in the proglacial areas. GPP changes react similarly to the different factors (Fig. 10c).

Similar findings have been identified in other alpine ecosystems. At an alpine treeline, climate warming rather than the rising atmospheric CO_2 level drove changes in the net CO_2 uptake rates, as treeline trees are not carbon limited (Wieser et al., 2019). However, in high alpine environments, CO_2 enrichment accelerated carbon cycling, leading to consistently increased carbon fixation, soil respiration, and dissolved organic carbon (Hättenschwiler et al., 2002; Dawes et al., 2013). During the process of wood encroachment, low temperature, instead of precipitation, served as the main limiting factor for vegetation NPP (Pellis et al., 2019). In nutrient-limited areas, insufficient nutrient availability might considerably constrain the carbon sink capacity (Goll et al., 2012; Wieder et al., 2015; Terrer et al., 2019).

4.3. Uncertainty estimation

We foresee that by the end of the century, NEP values would be around 24 gC m^{-2} y^{-1} for the RCP4.5 and 55 gC m^{-2} y^{-1} for the RCP8.5 (Fig. 8). Considering the internal climate variability and the climate model uncertainty, we can quantify the uncertainty range (i.e., the 5–95th percentiles) around these estimates to be in the order of ± 18 and ± 11 gC m^{-2} y^{-1} for the RCP4.5 and RCP8.5, respectively (Fig. 8). The level of uncertainty dictated by the various climate scenarios is relatively constrained, which enhances the degree of confidence in the NEP shifts.

Our analysis, however, does not consider several aspects (beyond climate) that may affect uncertainty estimations. First, we only considered the natural growth of plants in the conversion of bare soil, grass, and shrubs to forests; i.e., changes in vegetation fractions are limited to those types of vegetation currently present in the study area. Second, vegetation parameters, while constrained from observations in previous studies, are assumed to remain constant with a changing climate; several studies have shown that climate warming might alter plant functional traits (Mastrotheodoros et al., 2017; Bjorkman et al., 2018; Zhu et al., 2020; Wei et al., 2023). Third, we did not include any type of disturbance beyond background mortality, however, while infrequent in these Alpine ecosystems natural disturbances can be a noteworthy component of the carbon cycle (Pugh et al., 2019).

4.4. Increasing carbon sinks in Alpine proglacial areas and their implications

Glacier shrinkage and the consequent development of post-glacial ecosystems due to climate change represent some of the fastest ongoing ecosystem shifts (Bosson et al., 2023), characterized by rapid soil development and active plant colonization (Ficetola et al., 2024) and resulting in changes to the carbon dynamics of the newly deglaciated areas. Our findings support these statements and indicate that the ecosystems in the proglacial area we explored are projected to enhance their function as carbon sinks with climate change, with a rate stabilizing in the middle of the century (RCP4.5) or increasing up to the end of the century (RCP8.5).

Switzerland currently emits around 11.74 Mt C y^{-1} (Kemmler et al., 2021). The Swiss government has targeted reaching net-zero emissions by 2050, by reducing emissions from various sectors such as transportation, energy, and industry (Thalmann and Vielle, 2019; Kannan et al., 2022; Panos et al., 2023). Removing the natural intake of carbon

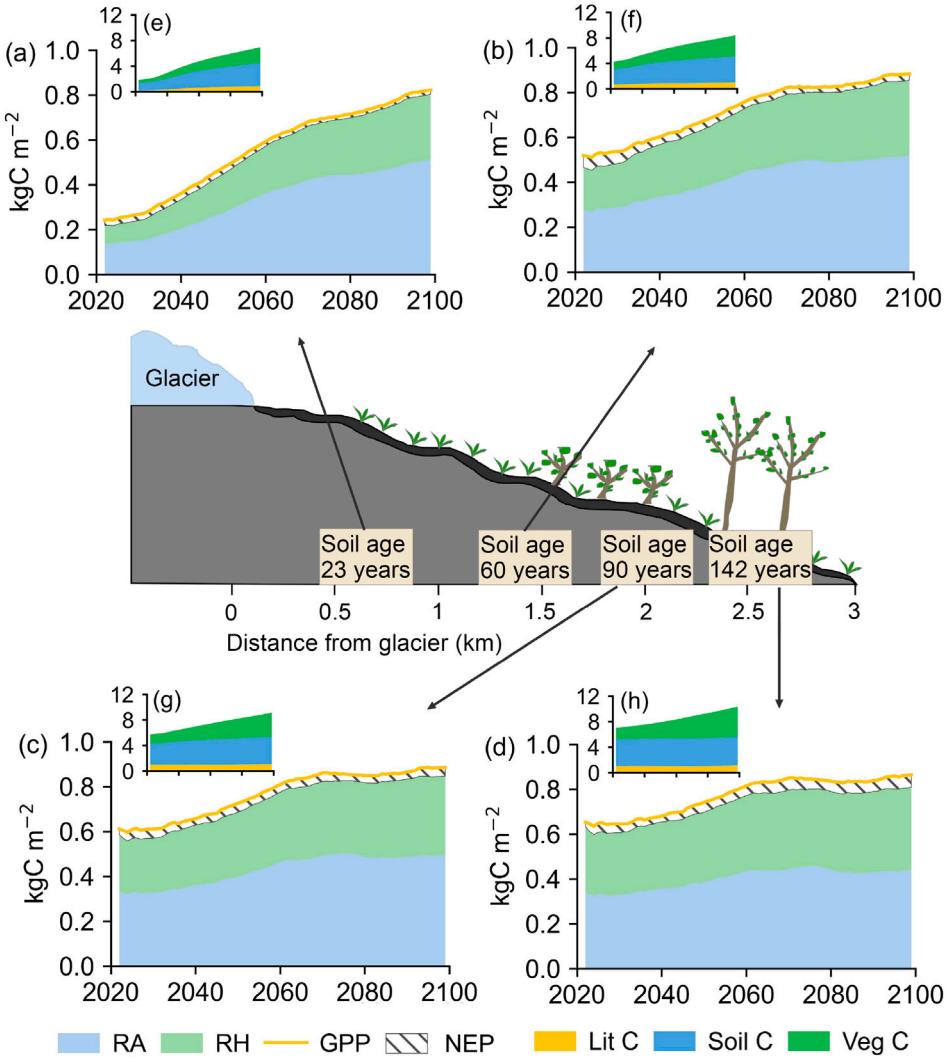

Fig. 9. Simulated trajectories during 2022–2099 of the carbon-balance variables (*NEP*, *RA*, *RH* and *GPP*) in the Ferpecle glacier foreland for sites of different soil ages (determined in 2022): (a) at 23-year-old sites, (b) at 60-year-old sites, (c) at 90-year-old sites, (d) at 142-year-old sites. Results are shown for the RCP4.5 scenario. Subplots (e, g, and h) present the same but for carbon pools (vegetation, soil, and litter).

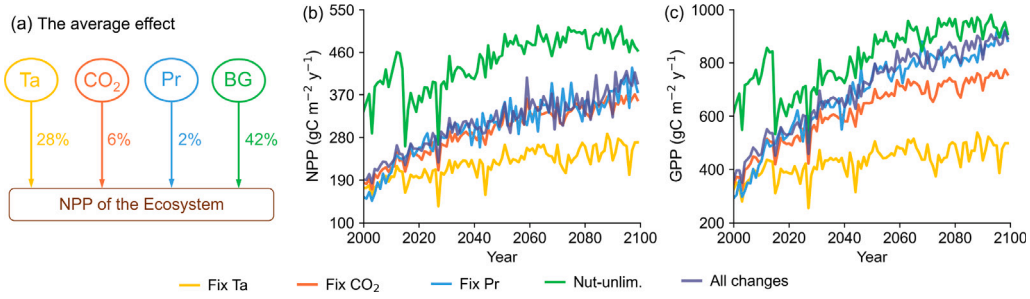

Fig. 10. (a) The average effects of air temperature (Ta), atmospheric CO_2 concentration (CO_2), precipitation (Pr), and soil nutrients (BG) to *NPP*, (b) *NPP* and (C) *GPP* for different simulation scenarios (Table 1) for the period 2000–2099 under RCP4.5.

in Switzerland, and the projected reduction in the energy, household, industry, and transportation emissions by 2050, implies that Swiss emissions should be further reduced by 3.19 Mt C (Kemmler et al., 2021) to reach the government goals.

Based on these premises, we assess the maximum potential contribution of carbon sinks emerging from proglacial areas in the Swiss Alps in the mid-century. Currently, there are around 161 large glaciers in Switzerland (Fig. 11), occupying an area of 961 km^2 in total. A few extreme assumptions are made: we assume that under the most extreme climate scenario (RCP8.5), all glaciers in the Swiss Alps will entirely disappear by 2050, that the *NEP* rate for mid-century computed for Ferpècle (Fig. 8) is representative for all proglacial areas in Switzerland, that forests are taking over in all locations similar to what projected above, and that the changes in climate conditions in all proglacial areas are similar as in our study area. With these assumptions, we compute the maximum potential carbon absorption by the ecosystems in all proglacial areas in 2050 to be 0.029 Mt C y^{-1}. Essentially, even in the absence of major disturbances, forest expansion in former glacier areas

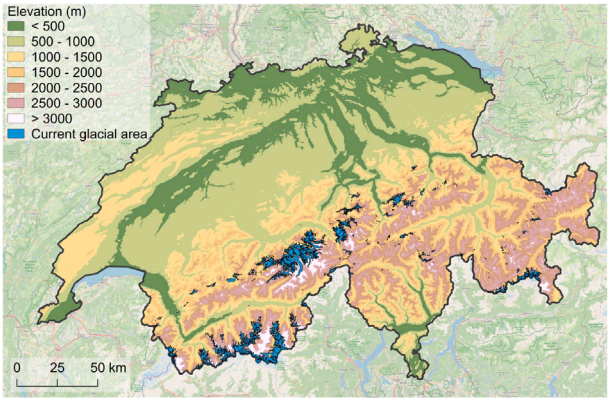

Fig. 11. Current glacial areas in the Swiss Alps.

will result in an increase in carbon sequestration that is only a drop in the ocean; just 0.9% of the carbon storage that is required to meet the net-zero emission target in Switzerland. Compared to current net CO_2 removals by Swiss forests at around 0.545 Mt C y^{-1} (Röthlisberger et al., 2024), this only accounts for 5.3%. However, when considering the total forest area at around 1.32×10^6 ha (Brändli et al., 2020), the carbon sink rate translates to 41.38 gC m^{-2}, which is comparable to the rate in deglaciated ecosystems. This limited carbon absorption capacity underscores the necessity for much more comprehensive climate actions, such as the transition to renewable energy sources, to achieve the net-zero target.

5. Conclusions

The results of this study, which employs a mechanistic ecohydrological model with a biogeochemistry module to compute carbon pools and fluxes from 1981 to 2099, show complex responses of the carbon cycle to a rapidly changing environment in a proglacial area located in the Swiss Alps. Following glacier retreat, newly exposed terrain allows for soil development and plant colonization. Plant growth experiences rapid accumulation of biomass, with NEP fluxes stabilizing after mid-century. Soil organic nutrients and plant nutrient uptake continue to rise by mid-century. Due to vegetation succession and soil development, the carbon stored in vegetation, soil, and litter is increasing, especially before mid-century, and only vegetation pools keep increasing rapidly thereafter. These changes will result in enhanced vegetation productivity, ecosystem respiration, and net ecosystem production. The ecosystems in the proglacial area are acting as carbon sinks, with sink strength potentially continuing to rise toward the end of the century, varying based on the climate change scenarios: around 24 ± 18 gC m^{-2} y^{-1} in RCP4.5 and 55 ± 11 gC m^{-2} y^{-1} in RCP8.5. Using Switzerland as a case study, we examined the implications of such increases in carbon storage on the national carbon budget. Even when extrapolating and generalizing these carbon sink rates assuming the most extreme case where all glaciers in Switzerland will be entirely disappear by mid-century, the maximum carbon absorption only accounts for 0.9% of Swiss carbon intake required to reach net-zero emissions. This highlights the limited potential of newly formed ecosystems to buffer against rising atmospheric CO_2, unless additional mitigation measures are implemented.

CRediT authorship contribution statement

Fuxiao Jiang: Writing – original draft, Methodology, Formal analysis, Conceptualization. **Simone Fatichi:** Writing – review & editing, Methodology, Conceptualization. **Gianalberto Losapio:** Writing – review & editing, Supervision, Data curation. **Nadav Peleg:** Writing – review & editing, Supervision, Methodology, Formal analysis.

Declaration of competing interest

The authors declare that they have no known competing financial interests or personal relationships that could have appeared to influence the work reported in this paper.

Acknowledgments

FJ acknowledges the support of the China Scholarship Council (CSC. Grant number: 202206040012). GL was supported by the Swiss National Science Foundation, Switzerland (PZ00P3_202127) and the Italian Ministry of University and Research (PRIN 2022 PNRR MITEX P2022N5KYJ). NP was supported by the Swiss National Science Foundation (SNSF), Switzerland, Grant 194649 ("Rainfall and floods in future cities"). We thank Cécile Charles and Stephanie Grand for helping with soil measurement data and Nora Khelidj and Natasha de Vere for helping with vegetation field data.

Appendix A. Supplementary data

Supplementary material related to this article can be found online at https://doi.org/10.1016/j.agrformet.2025.110682.

Data availability

Data will be made available on request.

References

Alves, M., Nadeau, D.F., Music, Biljana, Anctil, F., Fatichi, S., 2021. Can we replace observed forcing with weather generator in land surface modeling? Insights from long-term simulations at two contrasting boreal sites. Theor. Appl. Climatol. 145 (1), 215—244. http://dx.doi.org/10.1007/s00704-021-03615-y.

Bjorkman, A.D., Myers-Smith, I.H., Elmendorf, S.C., Normand, S., Rüger, N., Beck, P.S.A., Blach-Overgaard, A., Blok, D., Cornelissen, J.H.C., Forbes, B.C., Georges, D., Goetz, S.J., Guay, K.C., Henry, G.H.R., HilleRisLambers, J., Hollister, R.D., Karger, D.N., Kattge, J., Manning, P., Prevéy, J.S., Rixen, C., Schaepman-Strub, G., Thomas, H.J.D., Vellend, M., Wilmking, M., Wipf, S., Carbognani, M., Hermanutz, L., Lévesque, E., Molau, U., Petraglia, A., Soudzilovskaia, N.A., Spasojevic, M.J., Tomaselli, M., Vowles, T., Alatalo, J.M., Alexander, H.D., Anadon-Rosell, A., Angers-Blondin, S., Beest, M.t., Berner, L., Björk, R.G., Buchwal, A., Buras, A., Christie, K., Cooper, E.J., Dullinger, S., Elberling, B., Eskelinen, A., Frei, E.R., Grau, O., Grogan, P., Hallinger, M., Harper, K.A., Heijmans, M.M.P.D., Hudson, J., Hülber, K., Iturrate-Garcia, M., Iversen, C.M., Jaroszynska, F., Johnstone, J.F., Jørgensen, R.H., Kaarlejärvi, E., Klady, R., Kuleza, S., Kulonen, A., Lamarque, L.J., Lantz, T., Little, C.J., Speed, J.D.M., Michelsen, A., Milbau, A., Nabe-Nielsen, J., Nielsen, S.S., Ninot, J.M., Oberbauer, S.F., Olofsson, J., Onipchenko, V.G., Rumpf, S.B., Semenchuk, P., Shetti, R., Collier, L.S., Street, L.E., Suding, K.N., Tape, K.D., Trant, A., Treier, U.A., Tremblay, J.-P., Tremblay, M., Venn, S., Weijers, S., Zamin, T., Boulanger-Lapointe, N., Gould, W.A., Hik, D.S., Hofgaard, A., Jónsdóttir, I.S., Jorgenson, J., Klein, J., Magnusson, B., Tweedie, C., Wookey, P.A., Bahn, M., Blonder, B., van Bodegom, P.M., Bond-Lamberty, B., Campetella, G., Cerabolini, B.E.L., Chapin, F.S., Cornwell, W.K., Craine, J., Dainese, M., de Vries, F.T., Díaz, S., Enquist, B.J., Green, W., Milla, R., Niinemets, Ü., Onoda, Y., Ordoñez, J.C., Ozinga, W.A., Penuelas, J., Poorter, H., Poschlod, P., Reich, P.B., Sandel, B., Schamp, B., Sheremetev, S., Weiher, E., 2018. Plant functional trait change across a warming tundra biome. Nature 562 (7725), 57–62. http://dx.doi.org/10.1038/s41586-018-0563-7.

Bosson, J.B., Huss, M., Cauvy-Fraunié, S., Clément, J.C., Costes, G., Fischer, M., Poulenard, J., Arthaud, F., 2023. Future emergence of new ecosystems caused by glacial retreat. Nature 620 (7974), 562–569. http://dx.doi.org/10.1038/s41586-023-06302-2.

Botter, M., Zeeman, M., Burlando, P., Fatichi, S., 2021. Impacts of fertilization on grassland productivity and water quality across the European Alps under current and warming climate: insights from a mechanistic model. Biogeosciences 18 (6), 1917–1939. http://dx.doi.org/10.5194/bg-18-1917-2021.

Brändli, U.-B., Abegg, M., Leuch, B.A., 2020. Schweizerisches Landesforstinventar. Ergebnisse der vierten Erhebung 2009–2017. http://dx.doi.org/10.16904/envidat.146.

Brunner, M.I., Götte, J., Schlemper, C., Van Loon, A.F., 2023. Hydrological drought generation processes and severity are changing in the Alps. Geophys. Res. Lett. 50 (2), e2022GL101776. http://dx.doi.org/10.1029/2022GL101776.

Canedoli, C., Ferrè, C., Comolli, R., D'Amico, M.E., Rota, N., Abu El Khair, D., Padoa-Schioppa, E., 2024. Environmental factors influencing organic carbon stocks across different pools in alpine ecosystems. J. Mt. Sci. 21 (12), 4208–4222. http://dx.doi.org/10.1007/s11629-024-8657-1.

Cao, M., Woodward, F.I., 1998. Net primary and ecosystem production and carbon stocks of terrestrial ecosystems and their responses to climate change. Global Change Biol. 4 (2), 185–198. http://dx.doi.org/10.1046/j.1365-2486.1998.00125.x.

Chapin, F.S., Woodwell, G.M., Randerson, J.T., Rastetter, E.B., Lovett, G.M., Baldocchi, D.D., Clark, D.A., Harmon, M.E., Schimel, D.S., Valentini, R., Wirth, C., Aber, J.D., Cole, J.J., Goulden, M.L., Harden, J.W., Heimann, M., Howarth, R.W., Matson, P.A., McGuire, A.D., Melillo, J.M., Mooney, H.A., Neff, J.C., Houghton, R.A., Pace, M.L., Ryan, M.G., Running, S.W., Sala, O.E., Schlesinger, W.H., Schulze, E.-D., 2006. Reconciling carbon-cycle concepts, terminology, and methods. Ecosyst. 9 (7), 1041–1050. http://dx.doi.org/10.1007/s10021-005-0105-7.

Charles, C., Khelidj, N., Mottet, L., Tu, B.N., Adatte, T., Bomou, B., Faria, M., Monbaron, L., Reubi, O., de Vere, N., Grand, S., Losapio, G., 2024. Effects of glacier retreat on plant–soil relationships. Res. Sq. http://dx.doi.org/10.21203/rs.3.rs-4647918/v1.

Cheng, W., Dan, L., Deng, X., Feng, J., Wang, Y., Peng, J., Tian, J., Qi, W., Liu, Z., Zheng, X., Zhou, D., Jiang, S., Zhao, H., Wang, X., 2022. Global monthly gridded atmospheric carbon dioxide concentrations under the historical and future scenarios. Sci. Data 9 (1), 83. http://dx.doi.org/10.1038/s41597-022-01196-7.

D'Amico, M.E., Freppaz, M., Leonelli, G., Bonifacio, E., Zanini, E., 2015. Early stages of soil development on serpentinite: the proglacial area of the Verra Grande Glacier, Western Italian Alps. J. Soils Sediments 15 (6), 1292–1310. http://dx.doi.org/10.1007/s11368-014-0893-5.

Dang, C., Shao, Z., Huang, X., Zhuang, Q., Cheng, G., Qian, J., 2023. Climate warming-induced phenology changes dominate vegetation productivity in Northern Hemisphere ecosystems. Ecol. Indic. 151, 110326. http://dx.doi.org/10.1016/j.ecolind.2023.110326.

Darcy, J.L., Schmidt, S.K., Knelman, J.E., Cleveland, C.C., Castle, S.C., Nemergut, D.R., 2018. Phosphorus, not nitrogen, limits plants and microbial primary producers following glacial retreat. Sci. Adv. 4, eaaq0942. http://dx.doi.org/10.1126/sciadv.aaq0942.

Dawes, M.A., Hagedorn, F., Handa, I.T., Streit, K., Ekblad, A., Rixen, C., Körner, C., Hättenschwiler, S., 2013. An alpine treeline in a carbon dioxide-rich world: synthesis of a nine-year free-air carbon dioxide enrichment study. Oecologia 171 (3), 623–637. http://dx.doi.org/10.1007/s00442-012-2576-5.

De Kauwe, M.G., Medlyn, B.E., Zaehle, S., Walker, A.P., Dietze, M.C., Hickler, T., Jain, A.K., Luo, Y., Parton, W.J., Prentice, I.C., Smith, B., Thornton, P.E., Wang, S., Wang, Y.-P., W° arlind, D., Weng, E., Crous, K.Y., Ellsworth, D.S., Hanson, P.J., Seok Kim, H., Warren, J.M., Oren, R., Norby, R.J., 2013. Forest water use and water use efficiency at elevated: a model-data intercomparison at two contrasting temperate forest FACE sites. Global Change Biol. 19 (6), 1759–1779. http://dx.doi.org/10.1111/gcb.12164.

Delucia, E.H., Drake, J.E., Thomas, R.B., Gonzalez-Meler, M., 2007. Forest carbon use efficiency: is respiration a constant fraction of gross primary production? Global Change Biol. 13 (6), 1157–1167. http://dx.doi.org/10.1111/j.1365-2486.2007.01365.x.

Dümig, A., Smittenberg, R., Kögel-Knabner, I., 2011. Concurrent evolution of organic and mineral components during initial soil development after retreat of the damma glacier, Switzerland. Geoderma 163 (1), 83–94. http://dx.doi.org/10.1016/j.geoderma.2011.04.006.

Egli, M., Mavris, C., Mirabella, A., Giaccai, D., 2010. Soil organic matter formation along a chronosequence in the Morteratsch proglacial area (upper Engadine, Switzerland). CATENA 82 (2), 61–69. http://dx.doi.org/10.1016/j.catena.2010.05.001.

Fang, X., Zhao, L., Zhou, G., Huang, W., Liu, J., 2015. Increased litter input increases litter decomposition and soil respiration but has minor effects on soil organic carbon in subtropical forests. Plant Soil 392 (1), 139–153. http://dx.doi.org/10.1007/s11104-015-2450-4.

Fatichi, S., Ivanov, V.Y., 2014. Interannual variability of evapotranspiration and vegetation productivity. Water Resour. Res. 50 (4), 3275–3294. http://dx.doi.org/10.1002/2013WR015044.

Fatichi, S., Ivanov, V.Y., Caporali, E., 2011. Simulation of future climate scenarios with a weather generator. Adv. Water Resour. 34 (4), 448–467. http://dx.doi.org/10.1016/j.advwatres.2010.12.013.

Fatichi, S., Ivanov, V.Y., Caporali, E., 2012. A mechanistic ecohydrological model to investigate complex interactions in cold and warm water-controlled environments: 1. Theoretical framework and plot-scale analysis. J. Adv. Model. Earth Syst. 4 (2), M05002. http://dx.doi.org/10.1029/2011MS000086.

Fatichi, S., Ivanov, V.Y., Caporali, E., 2013. Assessment of a stochastic downscaling methodology in generating an ensemble of hourly future climate time series. Clim. Dyn. 40 (7), 1841–1861. http://dx.doi.org/10.1007/s00382-012-1627-2.

Fatichi, S., Ivanov, V.Y., Paschalis, A., Peleg, N., Molnar, P., Rimkus, S., Kim, J., Burlando, P., Caporali, E., 2016a. Uncertainty partition challenges the predictability of vital details of climate change. Earth' s Futur. 4 (5), 240–251. http://dx.doi.org/10.1002/2015EF000336.

Fatichi, S., Leuzinger, S., Paschalis, A., Langley, J.A., Barraclough, A.D., Hovenden, M.J., 2016b. Partitioning direct and indirect effects reveals the response of water-limited ecosystems to elevated CO2. PNAS 113 (45), 12757–12762. http://dx.doi.org/10.1073/pnas.1605036113.

Fatichi, S., Manzoni, S., Or, D., Paschalis, A., 2019. A mechanistic model of microbially mediated soil biogeochemical processes: a reality check. Glob. Biogeochem. Cycles 33 (6), 620–648. http://dx.doi.org/10.1029/2018GB006077.

Fatichi, S., Peleg, N., Mastrotheodoros, T., Pappas, C., Manoli, G., 2021. An ecohydrological journey of 4500 years reveals a stable but threatened precipitation–groundwater recharge relation around Jerusalem. Sci. Adv. 7 (37), eabe6303. http://dx.doi.org/10.1126/sciadv.abe6303.

Fatichi, S., Zeeman, M.J., Fuhrer, J., Burlando, P., 2014. Ecohydrological effects of management on subalpine grasslands: from local to catchment scale. Water Resour. Res. 50 (1), 148–164. http://dx.doi.org/10.1002/2013WR014535.

Ficetola, G.F., Marta, S., Guerrieri, A., Cantera, I., Bonin, A., Cauvy-Fraunié, S., Ambrosini, R., Caccianiga, M., Anthelme, F., Azzoni, R.S., Almond, P., Alviz Gazitúa, P., Ceballos Lievano, J.L., Chand, P., Chand Sharma, M., Clague, J.J., Cochachín Rapre, J.A., Compostella, C., Encarnación, R.C., Dangles, O., Deline, P., Eger, A., Erokhin, S., Franzetti, A., Gielly, L., Gili, F., Gobbi, M., Hågvar, S., Kaufmann, R., Khedim, N., Meneses, R.I., Morales-Martínez, M.A., Peyre, G., Pittino, F., Proietto, A., Rabatel, A., Sieron, K., Tielidze, L., Urseitova, N., Yang, Y., Zaginaev, V., Zerboni, A., Zimmer, A., Diolaiuti, G.A., Taberlet, P., Poulenard, J., Fontaneto, D., Thuiller, W., Carteron, A., 2024. The development of terrestrial ecosystems emerging after glacier retreat. Nature 632 (8024), 336–342. http://dx.doi.org/10.1038/s41586-024-07778-2.

Filippa, G., Cremonese, E., Galvagno, M., Isabellon, M., Bayle, A., Choler, P., Carlson, B.Z., Gabellani, S., Morra di Cella, U., Migliavacca, M., 2019. Climatic drivers of greening trends in the alps. Remote. Sens. 11 (21), http://dx.doi.org/10.3390/rs11212527.

Fischer, A., Fickert, T., Schwaizer, G., Patzelt, G., Groß, G., 2019. Vegetation dynamics in Alpine glacier forelands tackled from space. Sci. Rep. 9 (1), 13918. http://dx.doi.org/10.1038/s41598-019-50273-2.

Fischer, A., Strassmann, K., Croci-Maspoli, M., Hama, A., Knutti, R., Kotlarski, S., Schär, C., Schnadt Poberaj, C., Ban, N., Bavay, M., Beyerle, U., Bresch, D., Brönnimann, S., Burlando, P., Casanueva, A., Fatichi, S., Feigenwinter, I., Fischer, E., Hirschi, M., Liniger, M., Marty, C., Medhaug, I., Peleg, N., Pickl, M., Raible, C., Rajczak, J., Rössler, O., Scherrer, S., Schwierz, C., Seneviratne, S., Skelton, M., Sørland, S., Spirig, C., Tschurr, F., Zeder, J., Zubler, E., 2022. Climate scenarios for Switzerland CH2018 – approach and implications. Clim. Serv. 26, 100288. http://dx.doi.org/10.1016/j.cliser.2022.100288.

Fleischer, K., Terrer, C., 2022. Estimates of soil nutrient limitation on the CO fertilization effect for tropical vegetation. Global Change Biol. 28 (21), 6366–6369. http://dx.doi.org/10.1111/gcb.16377.

Friedlingstein, P., O'Sullivan, M., Jones, M.W., Andrew, R.M., Hauck, J., Landschützer, P., Le Quéré, C., Li, H., Luijkx, I.T., Olsen, A., Peters, G.P., Peters, W., Pongratz, J., Schwingshackl, C., Sitch, S., Canadell, J.G., Ciais, P., Jackson, R.B., Alin, S.R., Arneth, A., Arora, V., Bates, N.R., Becker, M., Bellouin, N., Berghoff, C.F., Bittig, H.C., Bopp, L., Cadule, P., Campbell, K., Chamberlain, M.A., Chandra, N., Chevallier, F., Chini, L.P., Colligan, T., Decayeux, J., Djeutchouang, L.M., Dou, X., Duran Rojas, C., Enyo, K., Evans, W., Fay, A.R., Feely, R.A., Ford, D.J., Foster, A., Gasser, T., Gehlen, M., Gkritzalis, T., Grassi, G., Gregor, L., Gruber, N., Gürses, Ö., Harris, I., Hefner, M., Heinke, J., Hurtt, G.C., Iida, Y., Ilyina, T., Jacobson, A.R., Jain, A.K., Jarníková, T., Jersild, A., Jiang, F., Jin, Z., Kato, E., Keeling, R.F., Klein Goldewijk, K., Knauer, J., Korsbakken, J.I., Lan, X., Lauvset, S.K., Lefèvre, N., Liu, Z., Liu, J., Ma, L., Maksyutov, S., Marland, G., Mayot, N., McGuire, P.C., Metzl, N., Monacci, N.M., Morgan, E.J., Nakaoka, S.-I., Neill, C., Niwa, Y., Nützel, T., Olivier, L., Ono, T., Palmer, P.I., Pierrot, D., Qin, Z., Resplandy, L., Roobaert, A., Rosan, T.M., Rödenbeck, C., Schwinger, J., Smallman, T.L., Smith, S.M., Sospedra-Alfonso, R., Steinhoff, T., Sun, Q., Sutton, A.J., Séférian, R., Takao, S., Tatebe, H., Tian, H., Tilbrook, B., Torres, O., Tourigny, E., Tsujino, H., Tubiello, F., van der Werf, G., Wanninkhof, R., Wang, X., Yang, D., Yang, X., Yu, Z., Yuan, W., Yue, X., Zaehle, S., Zeng, N., Zeng, J., 2025. Global carbon budget 2024. Earth Syst. Sci. Data 17 (3), 965–1039. http://dx.doi.org/10.5194/essd-17-965-2025.

Goll, D.S., Brovkin, V., Parida, B.R., Reick, C.H., Kattge, J., Reich, P.B., van Bodegom, P.M., Niinemets, Ü., 2012. Nutrient limitation reduces land carbon uptake in simulations with a model of combined carbon, nitrogen and phosphorus cycling. Biogeosciences 9 (9), 3547–3569. http://dx.doi.org/10.5194/bg-9-3547-2012.

Göransson, H., Welc, M., Bünemann, E.K., Christl, I., Venterink, H.O., 2016. Nitrogen and phosphorus availability at early stages of soil development in the damma glacier forefield, Switzerland; implications for establishment of N2-fixing plants. Plant Soil 404, 251–261. http://dx.doi.org/10.1007/s11104-016-2821-5.

Guelland, K., Hagedorn, F., Smittenberg, R.H., Göransson, H., Bernasconi, S.M., Hajdas, I., Kretzschmar, R., 2013. Evolution of carbon fluxes during initial soil formation along the forefield of damma glacier, Switzerland. Biogeochem. 113 (1), 545–561. http://dx.doi.org/10.1007/s10533-012-9785-1.

Guidi, C., Vesterdal, L., Gianelle, D., Rodeghiero, M., 2014. Changes in soil organic carbon and nitrogen following forest expansion on grassland in the southern Alps. For. Ecol. Manag. 328, 103–116. http://dx.doi.org/10.1016/j.foreco.2014.05.025.

Hättenschwiler, S., Handa, I.T., Egli, L., Asshoff, R., Ammann, W., Körner, C., 2002. Atmospheric CO2 enrichment of alpine treeline conifers. New Phytol. 156 (3), 363–375. http://dx.doi.org/10.1046/j.1469-8137.2002.00537.x.

Hersbach, H., Bell, B., Berrisford, P., Hirahara, S., Horányi, A., Muñoz-Sabater, J., Nicolas, J., Peubey, C., Radu, R., Schepers, D., Simmons, A., Soci, C., Abdalla, S., Abellan, X., Balsamo, G., Bechtold, P., Biavati, G., Bidlot, J., Bonavita, M., De Chiara, G., Dahlgren, P., Dee, D., Diamantakis, M., Dragani, R., Flemming, J., Forbes, R., Fuentes, M., Geer, A., Haimberger, L., Healy, S., Hogan, R.J., Hólm, E., Janisková, M., Keeley, S., Laloyaux, P., Lopez, P., Lupu, C., Radnoti, G., de Rosnay, P., Rozum, I., Vamborg, F., Villaume, S., Thépaut, J.-N., 2020. The ERA5 global reanalysis. Q. J. R. Meteorol. Soc. 146 (730), 1999–2049. http://dx.doi.org/10.1002/qj.3803.

Hiltbrunner, D., Zimmermann, S., Hagedorn, F., 2013. Afforestation with Norway spruce on a subalpine pasture alters carbon dynamics but only moderately affects soil carbon storage. Biogeochem. 115 (1), 251–266. http://dx.doi.org/10.1007/s10533-013-9832-6.

Hooker, T.D., Compton, J.E., 2003. Forest ecosystem carbon and nitrogen accumulation during the first century after agricultural abandonment. Ecol. Appl. 13 (2), 299–313. http://dx.doi.org/10.1890/1051-0761(2003)013[0299:FECANA]2.0.CO;2.

Huss, M., Hock, R., 2018. Global-scale hydrological response to future glacier mass loss. Nat. Clim. Chang. 8 (2), 135–140. http://dx.doi.org/10.1038/s41558-017-0049-x.

Ivanov, V.Y., Bras, R.L., Curtis, D.C., 2007. A weather generator for hydrological, ecological, and agricultural applications. Water Resour. Res. 43 (10), W10406. http://dx.doi.org/10.1029/2006WR005364.

Kannan, R., Panos, E., Hirschberg, S., Kober, T., 2022. A net-zero swiss energy system by 2050: technological and policy options for the transition of the transportation sector. Futur. Foresight Sci. 4 (3–4), e126. http://dx.doi.org/10.1002/ffo2.126.

Ke, P., Ciais, P., Sitch, S., Li, W., Bastos, A., Liu, Z., Xu, Y., Gui, X., Bian, J., Goll, D.S., Xi, Y., Li, W., O'Sullivan, M., de Souza, J.G., Friedlingstein, P., Chevallier, F., 2024. Low latency carbon budget analysis reveals a large decline of the land carbon sink in 2023. Natl. Sci. Rev. nwae367. http://dx.doi.org/10.1093/nsr/nwae367.

Kemmler, A., Kirchner, A., Kreidelmeyer, S., Piégsa, A., Spillmann, T., Dambeck, H., Falkenberg, H., Lübbers, S., Brutsche, A., Tschumi, D., Thurau, J., Ess, F., Thormeyer, C., Althaus, H.-J., Cox, B., Notter, B., Jakob, M., Reiter, U., Catenazzi, G., Sunarjo, B., Weinberg, L., Müller, J., Lienhard, L., 2021. Energy perspectives 2050+. URL https://www.bfe.admin.ch/bfe/en/home/policy/energy-perspectives-2050-plus.html/.

Khedim, N., Cécillon, L., Poulenard, J., Barré, P., Baudin, F., Marta, S., Rabatel, A., Dentant, C., Cauvy-Fraunié, S., Anthelme, F., Gielly, L., Ambrosini, R., Franzetti, A., Azzoni, R.S., Caccianiga, M.S., Compostella, C., Clague, J., Tielidze, L., Messager, E., Choler, P., Ficetola, G.F., 2021. Topsoil organic matter build-up in glacier forelands around the world. Global Change Biol. 27 (8), 1662–1677. http://dx.doi.org/10.1111/gcb.15496.

Knapp, A.K., Ciais, P., Smith, M.D., 2017. Reconciling inconsistencies in precipitation–productivity relationships: implications for climate change. New Phytol. 214 (1), 41–47. http://dx.doi.org/10.1111/nph.14381.

Kuemmerle, T., Olofsson, P., Chaskovskyy, O., Baumann, M., Ostapowicz, K., Woodcock, C.E., Houghton, R.A., Hostert, P., Keeton, W.S., Radeloff, V.C., 2011. Post-soviet farmland abandonment, forest recovery, and carbon sequestration in western Ukraine. Global Change Biol. 17 (3), 1335–1349. http://dx.doi.org/10.1111/j.1365-2486.2010.02333.x.

Lambiel, C., 2021. Glacial and periglacial landscapes in the Hérens Valley. In: Landscapes and Landforms of Switzerland. Springer International Publishing, Cham, pp. 263–275. http://dx.doi.org/10.1007/978-3-030-43203-4_18.

Li, F., Peng, Y., Zhang, D., Yang, G., Fang, K., Wang, G., Wang, J., Yu, J., Zhou, G., Yang, Y., 2019. Leaf area rather than photosynthetic rate determines the response of ecosystem productivity to experimental warming in an Alpine steppe. J. Geophys. Res.: Biogeosci. 124 (7), 2277–2287. http://dx.doi.org/10.1029/2019JG005193.

Liu, Y., Ji, M., Li, S., Ao, D., An, S., Liang, C., Liu, Y., 2024. Distinct contributions of microbial and plant residues to SOC during ecosystem primary succession in a tibetan glacier foreland. Appl. Soil Ecol. 203, 105675. http://dx.doi.org/10.1016/j.apsoil.2024.105675.

Losapio, G., Cerabolini, B.E.L., Maffioletti, C., Tampucci, D., Gobbi, M., Caccianiga, M., 2021. The consequences of glacier retreat are uneven between plant species. Front. Ecol. Evol. 8, http://dx.doi.org/10.3389/fevo.2020.616562.

Lucht, W., Prentice, I.C., Myneni, R.B., Sitch, S., Friedlingstein, P., Cramer, W., Bousquet, P., Buermann, W., Smith, B., 2002. Climatic control of the high-latitude vegetation greening trend and Pinatubo effect. Sci. 296 (5573), 1687–1689. http://dx.doi.org/10.1126/science.1071828.

Luo, X., Zhao, R., Chu, H., Collalti, A., Fatichi, S., Keenan, T., Lu, X., Nguyen, N., Prentice, I., Sun, W., Yu, L., 2025. Global variation in vegetation carbon use efficiency inferred from eddy covariance observations. Nat. Ecol. Evol. In press.

Manoli, G., Ivanov, V.Y., Fatichi, S., 2018. Dry-season greening and water stress in Amazonia: the role of modeling leaf phenology. J. Geophys. Res.: Biogeosci. 123 (6), 1909–1926. http://dx.doi.org/10.1029/2017JG004282.

Manzoni, S., Čapek, P., Porada, P., Thurner, M., Winterdahl, M., Beer, C., Brüchert, V., Frouz, J., Herrmann, A.M., Lindahl, B.D., Lyon, S.W., Šantrůčková, H., Vico, G., Way, D., 2018. Reviews and syntheses: carbon use efficiency from organisms to ecosystems – definitions, theories, and empirical evidence. Biogeosciences 15 (19), 5929–5949. http://dx.doi.org/10.5194/bg-15-5929-2018.

Mastrotheodoros, T., Pappas, C., Molnar, P., Burlando, P., Hadjidoukas, P., Fatichi, S., 2019. Ecohydrological dynamics in the Alps: insights from a modelling analysis of the spatial variability. Ecohydrol. 12 (1), e2054. http://dx.doi.org/10.1002/eco.2054.

Mastrotheodoros, T., Pappas, C., Molnar, P., Burlando, P., Keenan, T.F., Gentine, P., Gough, C.M., Fatichi, S., 2017. Linking plant functional trait plasticity and the large increase in forest water use efficiency. J. Geophys. Res.: Biogeosci. 122 (9), 2393–2408. http://dx.doi.org/10.1002/2017JG003890.

Mastrotheodoros, T., Pappas, C., Molnar, P., Burlando, P., Manoli, G., Parajka, J., Rigon, R., Szeles, B., Bottazzi, M., Hadjidoukas, P., Fatichi, S., 2020. More green and less blue water in the Alps during warmer summers. Nat. Clim. Chang. 10, 155–161. http://dx.doi.org/10.1038/s41558-019-0676-5.

Meinshausen, M., Vogel, E., Nauels, A., Lorbacher, K., Meinshausen, N., Etheridge, D.M., Fraser, P.J., Montzka, S.A., Rayner, P.J., Trudinger, C.M., Krummel, P.B., Beyerle, U., Canadell, J.G., Daniel, J.S., Enting, I.G., Law, R.M., Lunder, C.R., O'Doherty, S., Prinn, R.G., Reimann, S., Rubino, M., Velders, G.J.M., Vollmer, M.K., Wang, R.H.J., Weiss, R., 2017. Historical greenhouse gas concentrations for climate modelling (CMIP6). Geosci. Model. Dev. 10 (5), 2057–2116. http://dx.doi.org/10.5194/gmd-10-2057-2017.

Moustakis, Y., Fatichi, S., Onof, C., Paschalis, A., 2022. Insensitivity of ecosystem productivity to predicted changes in fine-scale rainfall variability. J. Geophys. Res.: Biogeosci. 127 (2), e2021JG006735. http://dx.doi.org/10.1029/2021JG006735.

Musso, A., Ketterer, M.E., Greinwald, K., Geitner, C., Egli, M., 2020. Rapid, decrease of soil erosion rates with soil formation and vegetation development in periglacial areas. Earth Surf. Process. Landforms 45 (12), 2824–2839. http://dx.doi.org/10.1002/esp.4932.

Nagler, M., Fontana, V., Lair, G.J., Radtke, A., Tasser, E., Zerbe, S., Tappeiner, U., 2015. Different management of larch grasslands in the European Alps shows low impact on above- and belowground carbon stocks. Agric. Ecosyst. Env. 213, 186–193. http://dx.doi.org/10.1016/j.agee.2015.08.005.

Nakatsubo, T., Bekku, Y.S., Uchida, M., Muraoka, H., Kume, A., Ohtsuka, T., Masuzawa, T., Kanda, H., Koizumi, H., 2005. Ecosystem development and carbon cycle on a glacier foreland in the high Arctic, Ny-Ålesund, Svalbard. J. Plant Res. 118 (3), 173–179. http://dx.doi.org/10.1007/s10265-005-0211-9.

Nissan, A., Alcolombri, U., Peleg, N., Galili, N., Jimenez-Martinez, J., Molnar, P., Holzner, M., 2023. Global warming accelerates soil heterotrophic respiration. Nat. Commun. 14 (1), 3452. http://dx.doi.org/10.1038/s41467-023-38981-w.

Pan, Y., Birdsey, R.A., Phillips, O.L., Houghton, R.A., Fang, J., Kauppi, P.E., Keith, H., Kurz, W.A., Ito, A., Lewis, S.L., Nabuurs, G.-J., Shvidenko, A., Hashimoto, S., Lerink, B., Schepaschenko, D., Castanho, A., Murdiyarso, D., 2024. The enduring world forest carbon sink. Nature 631 (8021), 563–569. http://dx.doi.org/10.1038/s41586-024-07602-x.

Pang, X., Fatichi, S., Lei, H., Cong, Z., Yang, H., Duan, L., 2023. Environmental changes promoted vegetation growth and reduced water yield over the temperate semi-arid grassland of China during 1901–2016. J. Hydrol. 618, 129235. http://dx.doi.org/10.1016/j.jhydrol.2023.129235.

Panos, E., Kannan, R., Hirschberg, S., Kober, T., 2023. An assessment of energy system transformation pathways to achieve net-zero carbon dioxide emissions in Switzerland. Commun. Earth Env. 4 (1), 157. http://dx.doi.org/10.1038/s43247-023-00813-6.

Paschalis, A., De Kauwe, M.G., Sabot, M., Fatichi, S., 2024. When do plant hydraulics matter in terrestrial biosphere modelling? Global Change Biol. 30 (1), e17022. http://dx.doi.org/10.1111/gcb.17022.

Paschalis, A., Fatichi, S., Zscheischler, J., Ciais, P., Bahn, M., Boysen, L., Chang, J., De Kauwe, M., Estiarte, M., Goll, D., Hanson, P.J., Harper, A.B., Hou, E., Kigel, J., Knapp, A.K., Larsen, K.S., Li, W., Lienert, S., Luo, Y., Meir, P., Nabel, J.E.M.S., Ogaya, R., Parolari, A.J., Peng, C., Peñuelas, J., Pongratz, J., Rambal, S., Schmidt, I.K., Shi, H., Sternberg, M., Tian, H., Tschumi, E., Ukkola, A., Vicca, S., Viovy, N., Wang, Y.-P., Wang, Z., Williams, K., Wu, D., Zhu, Q., 2020. Rainfall manipulation experiments as simulated by terrestrial biosphere models: where do we stand? Global Change Biol. 26 (6), 3336–3355. http://dx.doi.org/10.1111/gcb.15024.

Peleg, N., Molnar, P., Burlando, P., Fatichi, S., 2019. Exploring stochastic climate uncertainty in space and time using a gridded hourly weather generator. J. Hydrol. 571, 627–641. http://dx.doi.org/10.1016/j.jhydrol.2019.02.010.

Pellis, G., Chiti, T., Rey, A., Curiel Yuste, J., Trotta, C., Papale, D., 2019. The ecosystem carbon sink implications of mountain forest expansion into abandoned grazing land: the role of subsoil and climatic factors. Sci. Total Environ. 672, 106–120. http://dx.doi.org/10.1016/j.scitotenv.2019.03.329.

Peñuelas, J., Ciais, P., Canadell, J.G., Janssens, I.A., Fernández-Martínez, M., Carnicer, J., Obersteiner, M., Piao, S., Vautard, R., Sardans, J., 2017. Shifting from a fertilization-dominated to a warming-dominated period. Nat. Ecol. Evol. 1 (10), 1438–1445. http://dx.doi.org/10.1038/s41559-017-0274-8.

Piao, S., Ciais, P., Friedlingstein, P., de Noblet-Ducoudré, N., Cadule, P., Viovy, N., Wang, T., 2009. Spatiotemporal patterns of terrestrial carbon cycle during the 20th century. Glob. Biogeochem. Cycles 23 (4), GB4026. http://dx.doi.org/10.1029/2008GB003339.

Pörtner, H.-O., Roberts, D., Adams, H., Adelekan, I., Adler, C., Adrian, R., Aldunce, P., Ali, E., Begum, R.A., Friedl, B.B., Kerr, R.B., Biesbroek, R., Birkmann, J., Bowen, K., Caretta, M., Carnicer, J., Castellanos, E., Cheong, T., Chow, W., G. Cissé, G.C.,

Ibrahim, Z.Z., 2022. Climate change 2022: impacts, adaptation and vulnerability. Technical Summary, Cambridge University Press, Cambridge, UK and New York, USA, pp. 37–118. http://dx.doi.org/10.1017/9781009325844.

Pugh, T.A.M., Arneth, A., Kautz, M., Poulter, B., Smith, B., 2019. Important role of forest disturbances in the global biomass turnover and carbon sinks. Nat. Geosci. 12 (9), 730–735. http://dx.doi.org/10.1038/s41561-019-0427-2.

Ramirez, J.A., Peleg, N., Baird, A.J., Young, D.M., Morris, P.J., Larocque, M., Garneau, M., 2023. Modelling peatland development in high-boreal quebec, Canada, with DigiBog_boreal. Ecol. Model. 478, 110298. http://dx.doi.org/10.1016/j.ecolmodel.2023.110298.

Rangwala, I., Miller, J.R., 2012. Climate change in mountains: a review of elevation-dependent warming and its possible causes. Clim. Change 114 (3), 527–547. http://dx.doi.org/10.1007/s10584-012-0419-3.

Risch, A.C., Jurgensen, M.F., Page-Dumroese, D.S., Wildi, O., Schütz, M., 2008. Long-term development of above-and below-ground carbon stocks following land-use change in subalpine ecosystems of the Swiss National Park. Can. J. for. Res. 38 (6), 1590–1602. http://dx.doi.org/10.1139/X08-014.

Rogger, J., Hörtnagl, L., Buchmann, N., Eugster, W., 2022. Carbon dioxide fluxes of a mountain grassland: drivers, anomalies and annual budgets. Agric. for. Meteorol. 314, 108801. http://dx.doi.org/10.1016/j.agrformet.2021.108801.

Röthlisberger, R., Bass, A.-A., Schenker, S., Stettler, C., Bretscher, D., Schellenberger, A., Rihm, B., Rogiers, N., Leuenberger, D., Schilt, A., Guillevic, M., Bock, M., 2024. Switzerland's national inventory document 2024 (GHG inventory 1990–2022). URL https://www.bafu.admin.ch/bafu/en/home/topics/climate/state/data/climate-reporting/ghg-inventories/latest.html/.

Rumpf, S.B., Gravey, M., Brönnimann, O., Luoto, M., Cianfrani, C., Mariethoz, G., Guisan, A., 2022. From white to green: snow cover loss and increased vegetation productivity in the European Alps. Sci. 376 (6597), 1119–1122. http://dx.doi.org/10.1126/science.abn6697.

Schimel, D.S., 1995. Terrestrial ecosystems and the carbon cycle. Global Change Biol. 1 (1), 77–91. http://dx.doi.org/10.1111/j.1365-2486.1995.tb00008.x.

Smittenberg, R.H., Gierga, M., Göransson, H., Christl, I., Farinotti, D., Bernasconi, S.M., 2012. Climate-sensitive ecosystem carbon dynamics along the soil chronosequence of the damma glacier forefield, Switzerland. Global Change Biol. 18 (6), 1941–1955. http://dx.doi.org/10.1111/j.1365-2486.2012.02654.x.

Street, L.E., Shaver, G.R., Williams, M., VAN Wijk, M.T., 2007. What is the relationship between changes in canopy leaf area and changes in photosynthetic CO2 flux in arctic ecosystems? J. Ecol. 95 (1), 139–150. http://dx.doi.org/10.1111/j.1365-2745.2006.01187.x.

Stuart Chapin III, F., McFarland, J., David McGuire, A., Euskirchen, E.S., Ruess, R.W., Kielland, K., 2009. The changing global carbon cycle: linking plant–soil carbon dynamics to global consequences. J. Ecol. 97 (5), 840–850. http://dx.doi.org/10.1111/j.1365-2745.2009.01529.x.

Terrer, C., Jackson, R.B., Prentice, I.C., Keenan, T.F., Kaiser, C., Vicca, S., Fisher, J.B., Reich, P.B., Stocker, B.D., Hungate, B.A., Peñuelas, J., McCallum, I., Soudzilovskaia, N.A., Cernusak, L.A., Talhelm, A.F., Van Sundert, K., Piao, S., Newton, P.C.D., Hovenden, M.J., Blumenthal, D.M., Liu, Y.Y., Müller, C., Winter, K., Field, C.B., Viechtbauer, W., Van Lissa, C.J., Hoosbeek, M.R., Watanabe, M., Koike, T., Leshyk, V.O., Polley, H.W., Franklin, O., 2019. Nitrogen and phosphorus constrain the CO2 fertilization of global plant biomass. Nat. Clim. Chang. 9 (9), 684–689. http://dx.doi.org/10.1038/s41558-019-0545-2.

Thalmann, P., Vielle, M., 2019. Lowering CO 2 emissions in the swiss transport sector. Swiss J. Econ. Stat. 155, 1–12. http://dx.doi.org/10.1186/s41937-019-0037-3.

Thom, D., Seidl, R., 2022. Accelerating mountain forest dynamics in the Alps. Ecosystems 25 (3), 603–617. http://dx.doi.org/10.1007/s10021-021-00674-0.

Thuille, A., Schulze, E.-D., 2006. Carbon dynamics in successional and afforested spruce stands in Thuringia and the Alps. Global Change Biol. 12 (2), 325–342. http://dx.doi.org/10.1111/j.1365-2486.2005.01078.x.

Trautmann, S., Knoflach, B., Stötter, J., Elsner, B., Illmer, P., Geitner, C., 2023. Potential impacts of a changing cryosphere on soils of the European alps: A review. CATENA 232, 107439. http://dx.doi.org/10.1016/j.catena.2023.107439.

Tu, B.N., Khelidj, N., Cerretti, P., de Vere, N., Ferrari, A., Paone, F., Polidori, C., Schmid, J., Sommaggio, D., Losapio, G., 2024. Glacier retreat triggers changes in biodiversity and plant–pollinator interaction diversity. Alp. Bot. http://dx.doi.org/10.1007/s00035-024-00309-9.

Voicu, M.F., Shaw, C., Kurz, W.A., Huffman, T., Liu, J., Fellows, M., 2017. Carbon dynamics on agricultural land reverting to woody land in Ontario, Canada. J. Env. Manag. 193, 318–325. http://dx.doi.org/10.1016/j.jenvman.2017.02.019.

Wang, X., Liu, L., Piao, S., Janssens, I.A., Tang, J., Liu, W., Chi, Y., Wang, J., Xu, S., 2014. Soil respiration under climate warming: differential response of heterotrophic and autotrophic respiration. Global Change Biol. 20 (10), 3229–3237. http://dx.doi.org/10.1111/gcb.12620.

Wang, S., Zhang, Y., Ju, W., Chen, J.M., Ciais, P., Cescatti, A., Sardans, J., Janssens, I.A., Wu, M., Berry, J.A., Campbell, E., Fernández-Martínez, M., Alkama, R., Sitch, S., Friedlingstein, P., Smith, W.K., Yuan, W., He, W., Lombardozzi, D., Kautz, M., Zhu, D., Lienert, S., Kato, E., Poulter, B., Sanders, T.G.M., Krüger, I., Wang, R., Zeng, N., Tian, H., Vuichard, N., Jain, A.K., Wiltshire, A., Haverd, V., Goll, D.S., Peñuelas, J., 2020. Recent global decline of CO2 fertilization effects on vegetation photosynthesis. Sci. 370 (6522), 1295–1300. http://dx.doi.org/10.1126/science.abb7772.

Wei, B., Zhang, D., Wang, G., Liu, Y., Li, Q., Zheng, Z., Yang, G., Peng, Y., Niu, K., Yang, Y., 2023. Experimental warming altered plant functional traits and their coordination in a permafrost ecosystem. New Phytol. 240 (5), 1802–1816. http://dx.doi.org/10.1111/nph.19115.

Weiss, M., Baret, F., Jay, S., 2016. S2toolbox level 2 products: LAI, fapar, fcover. Inst. Natl. de la Rech. Agron. (INRA), Avignon URL https://step.esa.int/docs/extra/ATBD_S2ToolBox_L2B_V1.1.pdf.

Wieder, W.R., Cleveland, C.C., Smith, W.K., Todd-Brown, K., 2015. Future productivity and carbon storage limited by terrestrial nutrient availability. Nat. Geosci. 8 (6), 441–444. http://dx.doi.org/10.1038/ngeo2413.

Wieser, G., Oberhuber, W., Gruber, A., 2019. Effects of climate change at treeline: Lessons from space-for-time studies, manipulative experiments, and long-term observational records in the Central Austrian Alps. Forests 10 (6), http://dx.doi.org/10.3390/f10060508.

Williams, B.A., Beyer, H.L., Fagan, M.E., Chazdon, R.L., Schmoeller, M., Sprenkle-Hyppolite, S., Griscom, B.W., Watson, J.E.M., Tedesco, A.M., Gonzalez-Roglich, M., Daldegan, G.A., Bodin, B., Celentano, D., Wilson, S.J., Rhodes, J.R., Alexandre, N.S., Kim, D.-H., Bastos, D., Crouzeilles, R., 2024. Global potential for natural regeneration in deforested tropical regions. Nature 636 (8041), 131–137. http://dx.doi.org/10.1038/s41586-024-08106-4.

Xing, T., Liu, P., Ji, M., Deng, Y., Liu, K., Wang, W., Liu, Y., 2022. Sink or source: alternative roles of glacier foreland meadow soils in methane emission is regulated by glacier melting on the Tibetan Plateau. Front. Microbiol. 13, http://dx.doi.org/10.3389/fmicb.2022.862242.

Yang, D., Luo, J., Peng, P., Li, W., Shi, W., Jia, L., He, Y., 2021. Dynamics of nitrogen and phosphorus accumulation and their stoichiometry along a chronosequence of forest primary succession in the Hailuogou Glacier retreat area, eastern Tibetan Plateau. PLOS ONE 16, 1–16. http://dx.doi.org/10.1371/journal.pone.0246433.

Zaehle, S., Medlyn, B.E., De Kauwe, M.G., Walker, A.P., Dietze, M.C., Hickler, T., Luo, Y., Wang, Y.-P., El-Masri, B., Thornton, P., Jain, A., Wang, S., Warlind, D., Weng, E., Parton, W., Iversen, C.M., Gallet-Budynek, A., McCarthy, H., Finzi, A., Hanson, P.J., Prentice, I.C., Oren, R., Norby, R.J., 2014. Evaluation of 11 terrestrial carbon–nitrogen cycle models against observations from two temperate Free-Air CO2 Enrichment studies. New Phytol. 202 (3), 803–822. http://dx.doi.org/10.1111/nph.12697.

Zekollari, H., Huss, M., Farinotti, D., 2019. Modelling the future evolution of glaciers in the European Alps under the EURO-CORDEX RCM ensemble. Cryosphere 13 (4), 1125–1146. http://dx.doi.org/10.5194/tc-13-1125-2019.

Zemp, M., Haeberli, W., Hoelzle, M., Paul, F., 2006. Alpine glaciers to disappear within decades? Geophys. Res. Lett. 33 (13), http://dx.doi.org/10.1029/2006GL026319.

Zhang, J., Luo, J., DeLuca, T.H., Wang, G., Sun, S., Sun, X., Hu, Z., Zhang, W., 2021. Biogeochemical stoichiometry of soil and plant functional groups along a primary successional gradient following glacial retreat on the eastern Tibetan Plateau. Glob. Ecol. Conserv. 26, e01491. http://dx.doi.org/10.1016/j.gecco.2021.e01491.

Zhang, Y., Piao, S., Sun, Y., Rogers, B.M., Li, X., Lian, X., Liu, Z., Chen, A., Peñuelas, J., 2022. Future reversal of warming-enhanced vegetation productivity in the Northern Hemisphere. Nat. Clim. Chang. 12 (6), 581–586. http://dx.doi.org/10.1038/s41558-022-01374-w.

Zhu, Z., Piao, S., Myneni, R.B., Huang, M., Zeng, Z., Canadell, J.G., Ciais, P., Sitch, S., Friedlingstein, P., Arneth, A., Cao, C., Cheng, L., Kato, E., Koven, C., Li, Y., Lian, X., Liu, Y., Liu, R., Mao, J., Pan, Y., Peng, S., Peñuelas, J., Poulter, B., Pugh, T.A.M., Stocker, B.D., Viovy, N., Wang, X., Wang, Y., Xiao, Z., Yang, H., Zaehle, S., Zeng, N., 2016. Greening of the Earth and its drivers. Nat. Clim. Chang. 6 (8), 791–795. http://dx.doi.org/10.1038/nclimate3004.

Zhu, J., Zhang, Y., Yang, X., Chen, N., Li, S., Wang, P., Jiang, L., 2020. Warming alters plant phylogenetic and functional community structure. J. Ecol. 108 (6), 2406–2415. http://dx.doi.org/10.1111/1365-2745.13448.